

February 7, 2008
 UNITU-THEP-2/1999
 MIT-CTP-2807
 hep-ph/9902322

Nucleon Structure Functions in the Three Flavor NJL Soliton Model*

O. Schröder^a, H. Reinhardt^a and H. Weigel^{† a,b}

^aInstitute for Theoretical Physics, Tübingen University
 Auf der Morgenstelle 14, D-72076 Tübingen, Germany

^bCenter for Theoretical Physics
 Laboratory of Nuclear Science and Department of Physics
 Massachusetts Institute of Technology
 Cambridge, Ma 02139

ABSTRACT

We study the relevance of strange degrees of freedom for nucleon structure functions. For this purpose we employ the three flavor generalization of the collective quantization approach to the chiral soliton of the bosonized Nambu–Jona–Lasinio model. Contrary to many other soliton models the hadronic tensor is tractable in this model. By applying the Bjorken limit to the hadronic tensor we extract the leading twist contributions to the nucleon structure functions at the low energy scale at which the model is assumed to approximate QCD. After transforming to the infinite momentum frame and performing the DGLAP evolution program to these structure functions we compare with available data for deep inelastic electron–nucleon scattering.

PACS: 11.30.Cp, 12.39.Ki.

*This work is supported in parts by funds provided by the U.S. Department of Energy (D.O.E.) under cooperative research agreement #DF-FC02-94ER40818 and by the Deutsche Forschungsgemeinschaft (DFG) under contract We 1254/3-1 and the *Graduiertenkolleg Hadronen und Kerne* at Tübingen University.

[†]Heisenberg–Fellow

1. Introduction

In this paper we present the computation of the leading twist pieces of both the unpolarized and polarized nucleon structure functions in the three flavor Nambu–Jona–Lasino (NJL) [1] chiral soliton model [2, 3, 4]. Applying functional bosonization techniques [5] this model for the quark flavor dynamics can be straightforwardly expressed in terms of meson degrees of freedom. The identification of baryons as solitons of effective meson theories is motivated by generalizing quantum chromodynamics (QCD) to a large number (N_C) of color degrees of freedom [6]. Essentially this generalization shows that the baryon properties exhibit the same dependence on N_C as expected for soliton solutions of the effective meson theory. In addition to this analogy there are various reasons based on phenomenological observations to consider soliton models suitable for studying baryon properties. For example, such models quite successfully describe many aspects of static baryon properties [7, 8, 9, 10]. This is in particular the case for observables related to the *proton spin puzzle* [11] which is directly related to the polarized structure functions of the nucleon. Working in the three flavor extension of the model provides us with the advantageous feature of direct access to the strange quark contributions to structure functions even though the *net* strangeness of the nucleon vanishes. Hence we can gauge the importance of these degrees of freedom for dynamical properties of the nucleon. This is particularly interesting because the analyzes of experiments performed at CERN and SLAC have indicated that the spin of the strange quarks inside the nucleon yields a sizable contribution to the total nucleon spin.

Unfortunately there are a number of soliton models available. The reason for adopting the NJL chiral soliton model lies in the fact that the main ingredient in any structure function calculation is a bilocal commutator of hadronic currents as can be observed from the defining equation (24) of the hadronic tensor. It appears that its calculation in models with elementary meson fields is infeasible. However, it is much less involved in a model defined in terms of quark fields because the Compton amplitude, whose absorptive part equals this commutator, can be traced in the process of functional bosonization. Formally this process provides a unique regularization of the quark loop. Leaving aside the cumbersome issue of regularization in the NJL model, the leading twist contribution to the absorptive part of the Compton amplitude becomes as simple as a bilocal and bilinear operator of the quark fields.

In the present approach to the three flavor NJL–model we do not include the ’t Hooft determinant [12] which, when included [13], provides a mass for the singlet component of the η –meson and parameterizes the mixing of the uncharged pseudoscalar mesons. The reason for ignoring this piece of the action is that pseudoscalar flavor singlets couple only weakly to the chiral soliton, if at all [11]. In the soliton approach the influence of the ’t Hooft determinant on nucleon properties is hence negligible. It should however be remarked that at a sub–leading order in $1/N_C$ this term might give some contributions of the strange quarks to nucleon properties due to a mixing of non–strange and strange constituent quarks [14].

We should mention that there is an exhaustive number of model calculations for nucleon structure functions. The models applied range from various kinds of bag models [15, 16] over cloudy bag models [17] and meson cloud models [18] to (diquark) spectator models [19], just

to name a few. In the context of structure functions those model calculations may eventually be somewhat more reliable than soliton model results. After all, many of those models have particularly been set up to study structure functions. On the other hand soliton models are very attractive not only because of the above mentioned connection to QCD in the limit of large N_C and the possibility to generalize them to three flavors but over and above they provide a very comprehensive picture of baryons ranging way above static properties of nucleons from meson–nucleon scattering [20, 9] over systems with a heavy quark [21] to applications in the context of nuclear matter [22]. Thereby these models use only very a limited number of parameters. The present study apparently serves to further complete this comprehensive picture.

This paper is organized as follows: In section 2 we briefly review the NJL chiral soliton model and discuss the inclusion of strange degrees of freedom within the collective approach. Effects due to flavor symmetry breaking are incorporated into the collective nucleon wave–function by a generalization of the Yabu–Ando method [23, 10]. We then explain the calculation of the hadronic tensor for localized field configurations [15]. Employing pertinent projection techniques the structure functions are extracted from this tensor. In this section we furthermore include a brief discussion on the relevance of boosting to the infinite momentum frame [24, 25]. In the $1/N_C$ expansion scheme the dynamical response of the soliton to the momentum transfer is omitted which results in a violation of Lorentz covariance. Fortunately these omissions become irrelevant in the infinite momentum frame. We also discuss the valence quark approximation [26] to the structure function calculation which is to be considered as an approximation to avoid ambiguities inevitably arising when regularizing the vacuum part to bilocal–bilinear quark operators. Some of the previous approaches [27, 28] to the two flavor structure functions adopted a once–subtracted Pauli–Villars type scheme. This, however, is not sufficient to render finite the quadratic divergences contained in the model. As a consistent incorporation of flavor symmetry breaking in the three flavor model demands the solution of the quadratically divergent gap–equation a single subtraction will not be suited for present study¹. In section 3 we present our results for the unpolarized structure functions for both the electric and the strange current. Subsequently we discuss the polarized structure function g_1 in section 4. In particular we reflect on the electric and strange pieces in the light of the *proton spin puzzle*. In section 5 we will perform the DGLAP program to evolve the predicted structure functions from the low energy scale at which the model supposedly approximates QCD to the energy scale encountered in the respective experiments. In section 6 the numerical results will be presented and compared to data from CERN and SLAC experiments. Finally section 7 serves to summarize and conclude our study. Technicalities of the calculations are relegated to appendices.

Some of the results presented in this paper on the strangeness contribution to the polarized structure function $g_1(x)$ have already been published earlier [29].

¹In the case of the structure functions the absorptive part of the Compton amplitude – a matrix element of an operator which is quartic in the quark fields – appears to be the suitable starting point for a consistent regularization with two subtractions.

2. The Hadronic Tensor from The Chiral Soliton in the Three Flavor NJL Model

We split up this section into two pieces. In the first one we will review the treatment of the chiral soliton in the three flavor NJL model while the second one contains the discussion of the hadronic tensor $W_{\mu\nu}$ in this model.

2a. The Chiral Soliton in the Three Flavor NJL Model

The basis of our considerations is the NJL model Lagrangian [1]

$$\mathcal{L} = \bar{q}(i\cancel{\partial} - \hat{m}^0)q + 2G_{\text{NJL}} \sum_{i=0}^{N_f^2-1} \left((\bar{q}\frac{\lambda^i}{2}q)^2 + (\bar{q}\frac{\lambda^i}{2}i\gamma_5 q)^2 \right) \quad (1)$$

which is chirally symmetric for a vanishing current quark mass matrix \hat{m}^0 . In eq (1) q denotes the quark field. The matrices $\lambda^i/2$ are the generators of the flavor group $U(N_f)$. We will consider the case of three flavors ($N_f = 3$) and neglect isospin breaking, *i.e.* the current quark mass matrix acquires the form $\hat{m}^0 = \text{diag}(m^0, m^0, m_s^0)$ as $m^0 = m_u^0 = m_d^0$ is assumed. The NJL coupling constant G_{NJL} will later be determined from meson properties.

Applying functional integral bosonization techniques the model (1) can be rewritten in terms of composite meson fields [5]. The corresponding effective action is given by the sum $\mathcal{A}_{\text{NJL}} = \mathcal{A}_F + \mathcal{A}_m$ of a fermion determinant

$$\mathcal{A}_F = \text{Tr} \log(i\cancel{D}) = \text{Tr} \log \left(i\cancel{\partial} - (P_R M + P_L M^\dagger) \right) \quad (2)$$

and a purely mesonic part

$$\mathcal{A}_m = \int d^4x \left(-\frac{1}{4G_{\text{NJL}}} \text{tr}(M^\dagger M - \hat{m}^0(M + M^\dagger) + (\hat{m}^0)^2) \right). \quad (3)$$

Here $P_{R,L} = (1 \pm \gamma_5)/2$ denote the projectors onto right- and left-handed quark fields, respectively. The complex matrix $M = S + iP$ parameterizes the scalar and pseudoscalar meson fields.

Obviously, the action \mathcal{A}_F is quadratically divergent and needs to be regularized. We will apply the $O(4)$ invariant proper time regularization to \mathcal{A}_F in Euclidean space which then becomes a complex quantity $\mathcal{A}_F = \mathcal{A}_R + \mathcal{A}_I$. Proper time regularization amounts to replacing the real part of the fermion determinant \mathcal{A}_R by a parameter integral

$$\mathcal{A}_R = \frac{1}{2} \text{Tr} \log \left(\cancel{D}_E^\dagger \cancel{D}_E \right) \longrightarrow -\frac{1}{2} \int_{1/\Lambda^2}^{\infty} \frac{ds}{s} \text{Tr} \exp \left(-s \cancel{D}_E^\dagger \cancel{D}_E \right) \quad (4)$$

which becomes exact in the limit $\Lambda \rightarrow \infty$ up to an irrelevant additive constant. The imaginary part

$$\mathcal{A}_I = \frac{1}{2} \text{Tr} \log \left((\cancel{D}_E^\dagger)^{-1} \cancel{D}_E \right) \quad (5)$$

is finite and does not undergo regularization in order not to spoil the anomaly.

To study the three flavor extension of the model it is suitable to introduce the following parameterization for the meson fields

$$M = \xi \Sigma \xi. \quad (6)$$

The matrix Σ is Hermitian whereas ξ is unitary. In this parameterization the chiral $SU_L(3) \times SU_R(3)$ transformation $M \rightarrow LMR^\dagger$ with constant matrices L and R is realized via $\Sigma \rightarrow K\Sigma K^\dagger$ and $\xi \rightarrow L\xi K^\dagger = K\xi R^\dagger$. The latter equation determines the unitary matrix K [30].

Varying the action with respect to Σ yields the Schwinger–Dyson or gap equation which determines the vacuum expectation value (VEV), $\langle \Sigma \rangle = \text{diag}(m, m, m_s)$ and relates it to the quark condensate $\langle \bar{q}q \rangle_i$

$$m_i = m_i^0 + m_i^3 \frac{N_C G_{\text{NJL}}}{2\pi^2} \Gamma\left(-1, \left(\frac{m_i}{\Lambda}\right)^2\right) = m_i^0 - 2G_{\text{NJL}} \langle \bar{q}q \rangle_i. \quad (7)$$

Here $m_i = m, m_s$ denote the constituent masses of non-strange and strange quarks, respectively. The appearance of an incomplete Gamma-function of the order -1 reflects the fact that the model is quadratically divergent in the ultraviolet.

Space-time dependent fluctuating pseudoscalar meson fields $\eta_a(x)$ are introduced via

$$\xi_f(x) = \exp\left(i \sum_{a=1}^8 \eta_a(x) \lambda_a/2\right). \quad (8)$$

Expanding the effective action up to second order in the fluctuations $\eta_a(x)$ allows us (after rotating back to Minkowski space) to extract the inverse propagator for the pseudoscalar mesons

$$P_{ij} = \sum_{a=1}^{N_f^2-1} \eta^a \lambda_{ij}^a \quad [4]$$

$$D_{ij,kl}^{-1}(q^2) = \left(- \frac{(m_i^0 + m_j^0)(m_i + m_j)}{2G_{\text{NJL}}} - \Pi_{ij}(q^2) \right) \delta_{il} \delta_{kj}. \quad (9)$$

The polarization operator $\Pi_{ij}(q^2)$ is given by

$$\Pi_{ij}(q^2) = -2q^2 f_{ij}^2(q^2) + 2(m_i - m_j)^2 f_{ij}^2(q^2) - \frac{1}{2}(m_i^2 - m_j^2) \left(\frac{\langle \bar{q}q \rangle_i}{m_i} - \frac{\langle \bar{q}q \rangle_j}{m_j} \right) \quad (10)$$

wherein

$$f_{ij}^2(q^2) = \frac{1}{4}(m_i + m_j)^2 \frac{N_c}{4\pi^2} \int_0^1 dx \Gamma\left(0, [(1-x)m_i^2 + xm_j^2 - x(1-x)q^2]/\Lambda^2\right). \quad (11)$$

The Bethe–Salpeter equation $D^{-1}(q^2)P = 0$ which determines the physical meson masses m_{phys} is equivalent to the condition that the meson propagator acquires a pole:

$$\det\left(D_{ij,kl}^{-1}(q^2 = m_{\text{phys}}^2)\right) = 0. \quad (12)$$

Note that $f_{ij}^2(q^2 = m_{\text{phys}}^2)$ is the corresponding on-shell meson decay constant. From eq (11) we can read off the pion decay constant

$$f_\pi^2 = m^2 \frac{N_c}{4\pi^2} \int_0^1 dx \Gamma\left(0, [m^2 - x(1-x)m_\pi^2]/\Lambda^2\right) \quad (13)$$

Table 1: The up and strange quark constituent and current masses, the cutoff and the pion and the kaon decay constants for the parameters used later. Results are taken from ref [31].

m (MeV)	m_s (MeV)	m_s^0/m_u^0	Λ (MeV)	f_π (MeV)	f_K (MeV)
350	577	23.5	641	93.0	104.4
400	613	22.8	631	93.0	100.3
450	650	22.4	633	93.0	97.4
350	575	24.3	698	99.3	113.0
400	610	23.9	707	103.0	113.0
450	647	23.6	719	105.7	113.0

as well as the kaon decay constant

$$f_K^2 = \frac{1}{4}(m + m_s)^2 \frac{N_c}{4\pi^2} \int_0^1 dx \Gamma(0, [xm^2 + (1-x)m_s^2 - x(1-x)m_K^2]/\Lambda^2). \quad (14)$$

Using eqs (12,13) the four parameters of the model (1), the coupling constant G_{NJL} , the cutoff Λ and the two current masses m^0 and m_s^0 may be determined. The current quark masses are obtained from the pion and kaon masses, $m_\pi = 135$ MeV and $m_K = 495$ MeV. Fixing now the pion decay constant $f_\pi = 93$ MeV yields too small a value for the kaon decay constant, see table 1. On the other hand, requiring $f_K = 113$ MeV leaves us with too large a value for f_π .² In the following we will exclusively employ parameter sets which reproduce the physical value of f_π .

The expressions for the decay constants are only logarithmically divergent, which in a Pauli–Villars scheme could be cured by a single subtraction. For the full three flavor model this, however, would not be sufficient because the pertinent treatment of flavor symmetry breaking also requires the solution to the quadratically divergent gap–equation (7). In ref [32] the sizable effects of the second subtraction are discussed for meson observables which can be made finite by a single subtraction.

For the investigation of the baryon sector we constrain the meson fields to the chiral circle, *i.e.* we replace Σ by its VEV $\langle \Sigma \rangle$ in eq (6). Hence our NJL model soliton has the more complicated structure

$$M(\vec{x}) = \xi_0(\vec{x}) \langle \Sigma \rangle \xi_0(\vec{x}) \quad (15)$$

with

$$\xi_0(\vec{x}) = \begin{pmatrix} \exp[i\Theta(r)\hat{r} \cdot \vec{\tau}/2] & 0 \\ 0 & 1 \end{pmatrix} \quad (16)$$

containing the hedgehog *ansatz*. The computation of the classical energy associated with the

²Determining f_π or f_K fixes the ratio Λ/m . This leaves one adjustable parameter, *e.g.* the coupling constant G_{NJL} . However, as G_{NJL} is not very transparent we will use the gap equations (7) to re-express it in terms of the up constituent mass m .

unit baryon number sector of this field configuration is standard [33, 3]

$$E[\Theta] - E[\Theta = 0] = \frac{N_C}{2} \epsilon_V (1 + \text{sign}(\epsilon_V)) + \frac{N_C}{2} \int_{1/\Lambda^2}^{\infty} \frac{ds}{\sqrt{4\pi s^3}} \sum_{\nu} \exp(-s\epsilon_{\nu}^2) + m_{\pi}^2 f_{\pi}^2 \int d^3r [1 - \cos\Theta(r)], \quad (17)$$

where ϵ_{μ} are the eigenvalues of the single particle Dirac Hamiltonian

$$h_0 = \vec{\alpha} \cdot \vec{p} + m \beta \exp(i\gamma_5 \vec{\tau} \cdot \hat{r} \Theta(r)) \hat{T} + m_s \beta \hat{S} \quad (18)$$

In particular ϵ_V refers to the valence quark level which is strongly bound in background of the hedgehog. From the appearance of the strange and non-strange projectors $\hat{S} = \text{diag}_{\text{fl}}(0, 0, 1)$ and $\hat{T} = \text{diag}_{\text{fl}}(1, 1, 0)$ we observe that the strange quarks are not effected by the hedgehog field and hence obey a free Dirac equation. The profile of the chiral angle $\Theta(r)$ is determined by self-consistently minimizing the energy functional (17) [2, 34].

In order to generate states with baryon quantum numbers we apply the collective approach. In this approach time dependent coordinates $A(t) \in SU(3)$ which parameterize the orientation of the soliton in flavor space are introduced to approximate the unknown time dependent solution to the full equations of motion, *i.e.*

$$\xi(\vec{x}, t) = A(t) \xi_0(\vec{x}) A^{\dagger}(t). \quad (19)$$

The quantum mechanical treatment of these *would-be* zero-modes restores flavor covariance and due to the hedgehog *ansatz* also rotational covariance. Here we also recognize the advantage of the parameterization (6), as it avoids the time-dependent rotation of the flavor variant vacuum configuration, $\xi \equiv 1$. A slightly different parameterization for the flavor rotating meson fields is discussed in ref [35].

We now have to evaluate the action for the field configuration (19). This is most conveniently achieved by transforming to the flavor rotating frame $q' = A(t)q$ [33]. This transformation induces two additional pieces in the single particle Dirac Hamiltonian [4]

$$h = h_0 + h_{\text{rot}} + h_{\text{SB}} \quad (20)$$

which are due to the time dependence of the collective rotations

$$h_{\text{rot}} = -iA(t)^{\dagger} \dot{A}(t) = \sum_{a=1}^8 \Omega^a \frac{\lambda^a}{2}. \quad (21)$$

and the flavor symmetry breaking parameterized by the different constituent quark masses

$$h_{\text{SB}} = \mathcal{T} \beta \frac{m - m_s}{\sqrt{3}} (D_{8i} \lambda_i + D_{8\alpha} \lambda_{\alpha} + (D_{88} - 1) \lambda_8) \mathcal{T}^{\dagger}. \quad (22)$$

For convenience the angular velocities Ω_a and the chiral rotation $\mathcal{T} = \cos \frac{\Theta}{2} - i\gamma_5 \vec{\tau} \cdot \hat{r} \sin \frac{\Theta}{2}$ have been introduced. Furthermore the various isospin invariant components in h_{SB} have been

Table 2: The fermion contribution to the inertia parameter in the quantization rule (23). The moments of inertia α^2 and β^2 are given in GeV^{-1} while the coefficients α_1 and β_1 are dimensionless. The up-quark constituent mass m is in MeV. Note that when diagonalizing the collective Hamiltonian a piece ($\sim 1/\text{GeV}$) originating from induced kaon fields is augmented to the strange moment of inertia β^2 [4].

m	α_V^2	α_{vac}^2	α_{tot}^2	β_V^2	β_{vac}^2	β_{tot}^2	α_{1V}	$\alpha_{1\text{vac}}$	$\alpha_{1\text{tot}}$	β_{1V}	$\beta_{1\text{vac}}$	$\beta_{1\text{tot}}$
350	7.20	1.13	8.33	1.65	0.52	2.17	-0.925	-0.004	-0.929	-0.203	-0.003	-0.206
400	4.55	1.26	5.81	1.33	0.52	1.85	-0.401	-0.005	-0.405	-0.121	-0.003	-0.124
450	3.46	1.33	4.79	1.14	0.50	1.64	-0.232	-0.006	-0.238	-0.081	-0.004	-0.085

made explicit³. The modifications of the single particle Dirac Hamiltonian will be treated perturbatively since they are of sub-leading order either in $1/N_C$ or in $(m - m_s)/m$. Details of this calculation, which results in a Hamiltonian for the collective coordinates, may be traced from the literature [4]. The canonical momenta R_a appearing in this Hamiltonian are related to the angular velocities

$$R_a = \begin{cases} -(\alpha^2 \Omega_a + \alpha_1 D_{8a}), & a=1,2,3 \\ -(\beta^2 \Omega_a + \beta_1 D_{8a}), & a=4,\dots,7 \\ \frac{N_C B}{2\sqrt{3}}, & a=8 \end{cases} . \quad (23)$$

The inertia parameters α^2, \dots, β_1 are functionals of the soliton profile, again for explicit expressions we refer to the literature [3]. Furthermore $D_{ab} = (1/2)\text{tr}(\lambda_a A \lambda_b A^\dagger)$ denote the adjoint representation of the collective rotations. They appear in eq (23) as a consequence of flavor symmetry breaking, *i.e.* α_1 and β_1 are due to h_{SB} and hence proportional to the mass difference $m - m_s$. In table (2) we list the numerical values for these inertia parameters. In the process of quantization these canonical momenta are identified with the right generators of $SU(3)$. The resulting Hamiltonian $H(A, R)$ whose eigenstates are identified with the low-lying $\frac{1}{2}^+$ and $\frac{3}{2}^+$ baryons, also contains symmetry breaking terms. As a result of exactly diagonalizing $H(A, R)$ the $\frac{1}{2}^+$ baryons cease to be pure octet states, rather they contain sizable admixture of higher dimensional $SU(3)$ representations. Similarly the $\frac{3}{2}^+$ baryons are no pure decuplet states [26]. A major effect of these admixtures is to reduce the strange quark contributions to baryon properties, which are computed using the exact eigenfunctions of $H(A, R)$. This can easily be understood because due to the inclusion of symmetry breaking it is less probable for the heavier strange quarks to be excited. This effect will also become apparent in our results for the structure functions. Finally we should mention that the constraint for R_8 restricts the permissible $SU(3)$ representations to those containing only states with half-integer spins, *i.e.* fermions [36].

2b. The Hadronic Tensor in the NJL Chiral Soliton Model

³Throughout this paper we adopt the summation conventions $i, j, k, \dots = 1, 2, 3$ and $\alpha, \beta, \dots = 4, \dots, 7$.

The hadronic tensor which enters the cross-section of deep-inelastic scattering (DIS)

$$W_{\mu\nu}^{ab}(P, q; S) = \frac{1}{4\pi} \int d^4x e^{iq \cdot \xi} \langle P, S | [J_\mu^a(\xi), J_\nu^{b\dagger}(0)] | P, S \rangle \quad (24)$$

represents the defining quantity for the structure functions. They are certain combinations (see below) of the form factors appearing in the Lorentz-covariant decomposition (omitting parity violating contributions)

$$\begin{aligned} W_{\mu\nu}^{ab}(P, q; S) = & \left(-g_{\mu\nu} + \frac{q_\mu q_\nu}{q^2} \right) M_N W_1(x, Q^2) \\ & + \left(P_\mu - q_\mu \frac{P \cdot q}{q^2} \right) \left(P_\nu - q_\nu \frac{P \cdot q}{q^2} \right) \frac{1}{M_N} W_2(x, Q^2) \\ & + i\epsilon_{\mu\nu\lambda\sigma} \frac{q^\lambda M_N}{P \cdot q} \left([g_1(x, Q^2) + g_2(x, Q^2)] S^\sigma - \frac{q \cdot S}{q \cdot P} P^\sigma g_2(x, Q^2) \right). \end{aligned} \quad (25)$$

In eqs (24) and (25) the nucleon state is characterized by its momentum P and spin-orientation S . In the nucleon rest frame they are $P^\mu = (M_N, \vec{0})$ and $S^\mu = (0, \vec{s})$. The Lorentz-invariant quantities are the momentum transfer squared, $Q^2 = -q^2$ and the Bjorken variable $x = Q^2/2P \cdot q$ where q denotes the momentum of the exchanged boson. This boson couples to the hadronic current J_μ^a with a being a suitable flavor component⁴. Here it is important to note that this hadronic current is completely determined by the symmetry currents of QCD. Hence the hadronic current can unambiguously be computed in any model which has the same symmetries as QCD. This model current then completely saturates the hadronic tensor and at this point there is no need to identify the degrees of freedom of QCD within the model.

In the NJL model the interaction among the quarks does not contain any derivatives as can be seen from the defining equation (1). Hence the currents are formally identical to those of a free Dirac theory, *i.e.* $J_\mu^a = \bar{q} \gamma_\mu (\gamma_5) t^a q$ with t^a being a flavor generator. We will concentrate on the leading twist pieces of the structure functions. These are obtained from the Bjorken limit $-q^2, 2P \cdot q \rightarrow \infty$ with x fixed⁵. In this limit the computation of the hadronic tensor facilitates considerably since we may adopt the free correlation function for the highly off-shell intermediate quark propagating between the two boson insertions:

$$\begin{aligned} W_{\mu\nu}^{ab}(P, q; S) = & \frac{1}{4\pi} \int d^4\xi e^{iq \cdot \xi} \int \frac{d^4k}{(2\pi)^4} e^{ik \cdot \xi} \text{sign}(k_0) 2\pi \delta(k^2) \\ & \times \langle P, S | \bar{q}(\xi) \gamma_\mu t^a \not{k} t^b \gamma_\nu q(0) - \bar{q}(0) \gamma_\nu t^b \not{k} t^a \gamma_\mu q(\xi) | P, S \rangle. \end{aligned} \quad (26)$$

Apparently the hadronic tensor acquires contributions from intermediate quarks propagating in forward ($\xi \rightarrow 0$) and backward ($0 \rightarrow \xi$) directions. In order to apply this formalism to the soliton configuration, which breaks translational invariance, we still need to generate states of good linear momentum. This is essentially done in the same way as the flavor-spin projection

⁴We omit the flavor indices of the form factors.

⁵That is, the higher order contributions in $1/Q^2$ are dropped. The logarithmic dependence on Q^2 originating from perturbative gluon emission to the nucleon will be discussed in section 5.

discussed previously by introducing a collective coordinate \vec{R} describing the position of the classical soliton in coordinate space. As the nucleons in the *bra* and *ket* states have the same momenta this boils down to an additional integral in coordinates space yielding [15]

$$W_{\mu\nu}^{ab}(P, q; S) = \frac{M_N}{(2\pi)^4} \int dt d^3\xi_1 d^3\xi_2 \int d^4k \text{sign}(k_0) \delta(k^2) e^{i(q_0+k_0)t - i(\vec{q}+\vec{k})\cdot(\vec{\xi}_1-\vec{\xi}_2)} \\ \times \langle N | \bar{q}(\vec{\xi}_1, t) \gamma_\mu t^a \not{k} t^b \gamma_\nu q(\vec{\xi}_2, 0) - \bar{q}(\vec{\xi}_2, 0) \gamma_\nu t^b \not{k} t^a \gamma_\mu q(\vec{\xi}_1, t) | N \rangle. \quad (27)$$

Here, $|N\rangle$ is defined via $\langle \vec{R} | P, S \rangle = \sqrt{2E} \exp(i\vec{P} \cdot \vec{R}) | N \rangle$. Although this now is a simplified version of the hadronic tensor it is not well suited for the ongoing calculation in the bosonized NJL model. The main reason is that the matrix element to be computed is that of a bilocal and bilinear quark operator which appears as an ordinary product rather than a time-ordered product. Only the latter would be suitable to undergo the bosonization procedure which in turn could provide a rigorous regularization of the structure functions consistent with the meson sector of the model as well as other soliton calculations. One possible way to achieve that goal would be to start from the forward Compton amplitude whose absorptive part is identical to the hadronic tensor. This amplitude is calculated as the matrix element of the time-ordered product of the electromagnetic currents and can hence straightforwardly be implemented in the functional bosonization thereby implementing a unique regularization. Although first results [37] in this direction are promising⁶ we will presently avoid the ambiguities connected with regularizing structure functions by employing the valence quark approximation. This approximation consists of substituting the valence quark wave-function

$$q(\vec{\xi}, t) = \psi_V(\vec{\xi}, t) = e^{-i\epsilon_V t} A(t) \left(\Psi_V(\vec{\xi}) + \sum_{\nu \neq V} \Psi_\nu(\vec{\xi}) \frac{\langle \nu | h_{\text{rot}} + h_{\text{SB}} | V \rangle}{\epsilon_V - \epsilon_\nu} \right) \quad (28)$$

in the above expression for the hadronic tensor (27). The main arguments to consider this valence quark approximation to be reliable are the facts that the valence quark contribution does not undergo regularization in any event and the observation that this level dominates the results for the static properties. The axial properties are actually almost saturated by the valence quark contribution [3]. It is important to note that this valence level should not be confused with the valence quark in the parton model description of the structure functions. Here it rather refers to the distinct quark state which is strongly bound in the soliton background.

Note that both the rotational and symmetry breaking corrections have been included. This, of course, is necessary in order to disentangle various flavor contributions. Consistent $1/N_C$ counting makes it necessary to consider the time-dependence of A [39]. This additional bilocality in the time coordinates is treated in an $1/N_C$ expansion employing the quantization rules (23)

$$A(t) = A(t_0) + (t - t_0) \frac{dA(t)}{dt} \Big|_{t=t_0} + \mathcal{O}\left(\frac{1}{N_C^2}\right)$$

⁶Since the incomplete gamma-functions appearing in the proper-time regularization have various unphysical poles in the complex plane it is more appropriate to employ the Pauli-Villars regularization when identifying the cuts of the Compton amplitude [38]. In contrast to earlier two flavor calculations of the structure functions, which only included a single subtraction [27, 28, 39], the computation of the Compton amplitude allows one to consistently incorporate the two subtractions demanded by the quadratically divergent gap-equation.

$$= A(t_0) + \frac{i}{2}(t - t_0)A(t_0) \sum_{a=1}^8 \lambda^a \Omega_a(t_0) + \dots, \quad (29)$$

where the ellipsis refer to higher order contributions in the angular velocities which according to eq (23) correspond to higher orders in $1/N_C$ and/or flavor symmetry breaking. At this point we recognize that the computation of nucleon matrix elements associated with the expansion (29) will also demand the matrix element of Ω_8 . This component of the angular velocity is not provided by the quantization prescription (23). We obtain the relevant information from

$$\Omega_8 = -i \text{tr} \left(\lambda^8 A(t)^\dagger \dot{A}(t) \right) = \text{tr} \left(\lambda^8 A(t) [H, A(t)] \right), \quad (30)$$

with $H = H(A, R)$ being the Hamilton operator for the collective coordinates, its eigenstates are the baryons, *cf.* the discussion after eq (23). Employing the defining equation for right generators, *i.e.* $[A, R_a] = A\lambda_a/2$ yields

$$\langle \Omega_8 \rangle = \frac{\sqrt{3}}{4\alpha^2} - \frac{1}{2\sqrt{3}\beta^2}. \quad (31)$$

It is straightforward to verify that the application of the same procedure to $\Omega_1, \dots, \Omega_7$ is consistent with the quantization rules (23).

3. Unpolarized Nucleon Structure Functions

We have now collected all ingredients necessary to apply the valence quark approximation to the computation of the hadronic tensor in the NJL chiral soliton model. In a first step we project the unpolarized structure function $f_1(x)$ from $W_{\mu\nu}$ by contracting it appropriately with

$$\Lambda_{f_1}^{\mu\nu} = \frac{1}{2}(-g^{\mu\nu} + \frac{\eta}{M_N^2} P^\mu P^\nu) \quad \text{where} \quad \eta = \left(1 + \frac{P \cdot q}{2xM_N^2} \right)^{-1}. \quad (32)$$

In the Bjorken limit, which in the nucleon rest frame $P^\mu = (M_N, \vec{0})^\mu$ is implemented via

$$q_0 = |\vec{q}| - xM_N \quad \text{with} \quad |\vec{q}| \rightarrow \infty, \quad (33)$$

the leading twist pieces of the structure functions are extracted. In this limit this projector becomes as simple as $-g^{\mu\nu}/2$ when contracted with the hadronic tensor in the form of eq (27). In this limit the evaluation of the contribution due to the bilocality in the time-coordinate (29) also becomes feasible. The linear t -dependence is treated as a derivative with respect to q^0 . The q^0 dependence of the structure functions occurs via the Bjorken variable x . Hence this derivative is replaced by $\frac{-1}{M_N} \frac{d}{dx}$. Accordingly it is convenient to separate the unpolarized structure function f_1 into two contributions:

$$f_1(x) = \tilde{f}_1(x) + \Delta f_1(x) \quad (34)$$

with $\Delta f_1(x)$ containing the piece due to bilocality in the collective coordinates (29). By definition this contribution is already linear in the angular velocities, and hence of sub-leading

order. Consequently the structure function $\Delta f_1(x)$ is completely given in terms of the classical fields, *i.e.* by omitting the cranking correction in eq (28).

It is henceforth useful to define the following Fourier-transformations

$$\tilde{\psi}_V(\vec{p}) = \int \frac{d^3\xi}{4\pi} \left(\Psi_V(\vec{\xi}) + \sum_{\nu \neq V} \Psi_\nu(\vec{\xi}) \frac{\langle \nu | h_{\text{rot}} + h_{\text{SB}} | V \rangle}{\epsilon_V - \epsilon_\nu} \right) \exp(i\vec{\xi} \cdot \vec{p}) \quad (35)$$

and

$$\tilde{\Psi}_V(\vec{p}) = \int \frac{d^3\xi}{4\pi} \Psi_V(\vec{\xi}) \exp(i\vec{\xi} \cdot \vec{p}) . \quad (36)$$

According to eq (27) we put $\vec{p} = \vec{k} + \vec{q}$ together with the on-shell condition $k = |\vec{k}| = q_0 \mp \epsilon_V$ pertinent for the forward and backward contributions to the hadronic tensor. As in the Bjorken limit q_0 tends to infinity and $q_0 - k$ remains finite, we may change the integration measure to

$$k^2 d\Omega_{\vec{k}} = p dp d\phi \quad (37)$$

with $p = |\vec{p}|$ and ϕ being the azimuth angle between \vec{q} and \vec{p} . The lower limit of the p -integration is assumed when \vec{k} and \vec{q} are anti-parallel, *i.e.* $p_{\pm}^{\text{min}} = |M_N x \mp \epsilon_V| =: M_N |x_{\mp}|$. Finally we make use of the single quark wave-function containing only finite momentum modes of the order $p \approx \epsilon_V$. Hence the integral receives non-vanishing contributions only when $\hat{k} = -\hat{q}$ [15, 26]. With these preliminaries the unpolarized structure function f_1 becomes

$$\begin{aligned} \tilde{f}_1^{ab} &= N_C \frac{M_N}{\pi} \langle N | \int_{M_N |x_-|}^{\infty} p dp d\phi \tilde{\psi}_V^\dagger(\vec{p}_-) (1 - \vec{\alpha} \cdot \hat{q}) A^\dagger \mathcal{O}^{ba} A \tilde{\psi}_V(\vec{p}_-) \\ &\quad - \int_{M_N |x_+|}^{\infty} p dp d\phi \tilde{\psi}_V^\dagger(\vec{p}_+) (1 + \vec{\alpha} \cdot \hat{q}) A^\dagger \mathcal{O}^{ab} A \tilde{\psi}_V(\vec{p}_+) | N \rangle \\ &= \tilde{f}_{1,-}^{ab} - \tilde{f}_{1,+}^{ab} \end{aligned} \quad (38)$$

$$\begin{aligned} \Delta f_1^{ab} &= -\frac{N_C}{2\pi} \frac{d}{dx} \langle N | \int_{M_N |x_-|}^{\infty} p dp d\phi \tilde{\Psi}_V^\dagger(\vec{p}_-) (1 - \vec{\alpha} \cdot \hat{q}) A^\dagger \mathcal{O}^{ba} A \Omega_g \lambda^g \tilde{\Psi}_V(\vec{p}_-) \\ &\quad + \int_{M_N |x_+|}^{\infty} p dp d\phi \tilde{\Psi}_V^\dagger(\vec{p}_+) (1 + \vec{\alpha} \cdot \hat{q}) \Omega_g \lambda^g A^\dagger \mathcal{O}^{ab} A \tilde{\Psi}_V(\vec{p}_+) | N \rangle \\ &= \Delta f_{1,-}^{ab} + \Delta f_{1,+}^{ab} \end{aligned} \quad (39)$$

where we have also used that the valence quark wave-function carries positive parity, *i.e.* $\psi_V(-\vec{p}) = \gamma_0 \psi_V(\vec{p})$. The momentum \vec{p}_{\pm} denotes the integrated momentum with the polar angle fixed, $\cos\Theta^{\pm} = M_N x_{\pm}/p$. The flavor structure of the integrand is now comprised in the matrices $\mathcal{O}^{ab} = t^a t^b$ which are diagonal for all processes in which we are interested

$$\begin{aligned} \mathcal{O}^{ab} &= \delta_0 \mathbf{1} + \delta_3 \lambda_3 + \delta_8 \lambda_8 \\ \mathcal{O}^{ba} &= \delta'_0 \mathbf{1} + \delta'_3 \lambda_3 + \delta'_8 \lambda_8 . \end{aligned} \quad (40)$$

These matrices are given by the physical process under consideration as this specifies the flavor matrices t^a and t^b in the hadronic tensors. Since we will ignore Cabbibo mixing, the two sets $(\delta_0, \delta_3, \delta_8)$ and $(\delta'_0, \delta'_3, \delta'_8)$ differ at most by the sign of δ_3 and δ'_3 .

We remark the change of sign in the backward moving quark contribution when going from \tilde{f}_1 to Δf_1 . This stems from the different expansion (29) caused by exchanging the time arguments of the collective coordinates.

According to the quantization rule (23) the collective coordinates and their time derivatives Ω_a are elevated to non-commuting operators. Guided by symmetry requirements such as hermiticity, PCAC and G-parity we adopt the symmetric ordering whenever ambiguities occur⁷, *i.e.* $D_{ab}\Omega_c \rightarrow \{D_{ab}, \Omega_c\}/2$.

For a consistent formulation of the valence quark approximation we consider the sum rules for isospin and strangeness of the nucleon. The former is known as the Adler sum rule and refers to (anti)-neutrino scattering off the nucleon. For these processes we require $t^a = (t^b)^\dagger = (\lambda^1 \pm i\lambda^2)$. According to eq (40) the subtraction of neutrino and anti-neutrino scattering processes⁸

$$\int \frac{dx}{x} (f_2^{\bar{\nu}N} - f_2^{\nu N}) \quad (41)$$

corresponds to $\delta_3 = -\delta'_3 = 1$ with all other $\delta_a^{(\prime)}$ s identical to zero. It is then straightforward to verify that

$$\int dx (\tilde{f}_{1,-} - \tilde{f}_{1,+}) = \langle N | 2I_3 | N \rangle \quad (42)$$

$$\int dx (\Delta f_{1,-} + \Delta f_{1,+}) = 0 \quad (43)$$

with $I_3 = D_{3i}R_i + D_{3\alpha}R_\alpha + D_{38}R_8$. However, for eq (42) to be valid, we have to restrict the inertial parameters appearing in the quantization rule (23) to their dominating valence quark contribution. Of course, this is expected. The differences between using the total values of these inertial parameters and these valence quark contributions can be employed to estimate the uncertainties of the valence quark approximation. Within the same restriction also the strangeness sum rule for $t^a = t^b = (1 - \sqrt{3}\lambda^8)/3$ holds as one easily verifies that (for $N_C = 3$)

$$\int dx (\tilde{f}_{1,-} + \tilde{f}_{1,+}) = \frac{-1}{2} \langle N | \hat{S} | N \rangle \quad (44)$$

$$\int dx (\Delta f_{1,-} - \Delta f_{1,+}) = 0 \quad (45)$$

with $\hat{S} = (2\sqrt{3}/N_C)(L_8 - R_8)$. An interesting sum rule for the unpolarized structure functions is the so-called Gottfried sum rule [41] which addresses electron-nucleon scattering,

$$S_G = \int \frac{dx}{x} (f_2^{\text{ep}} - f_2^{\text{en}}). \quad (46)$$

⁷While G-parity invariance can be maintained for other orderings when going beyond the valence quark approximation this is not the case for PCAC [40].

⁸Here we do not specify the boundaries of the integrals because they will be subject to the boost into the infinite momentum frame, *cf.* eq (59).

The structure function f_2 is related to the form factor W_2 in the defining equation (25) by $f_2 = -q^2 W_2 / 2M_N x$. In the Bjorken limit the Callan Gross relation $f_2 = 2x f_1$ is identically fulfilled. Using the electromagnetic combination

$$\mathcal{O}^{ab} = \mathcal{O}^{ba} = (\lambda_3/2 + \lambda_8/2\sqrt{3})^2 =: \mathcal{O}^{\text{e.m.}} \quad (47)$$

we therefore find

$$S_G = 2 \frac{N_C}{3\pi} \int dx (s_G(x) + \Delta s_G(x)) \quad (48)$$

with

$$\begin{aligned} s_G(x) = & M_N \langle N | \int_{M_N|x_-}^{\infty} pdpd\phi \tilde{\psi}_V^\dagger(\vec{p}_-)(1 - \vec{\alpha} \cdot \hat{q}) A^\dagger \lambda_3 A \tilde{\psi}_V(\vec{p}_-) \\ & - \int_{M_N|x_+}^{\infty} pdpd\phi \tilde{\psi}_V^\dagger(\vec{p}_+)(1 + \vec{\alpha} \cdot \hat{q}) A^\dagger \lambda_3 A \tilde{\psi}_V(\vec{p}_+) | N \rangle \end{aligned}$$

and

$$\begin{aligned} \Delta s_G(x) = & -\frac{1}{2} \frac{d}{dx} \langle N | \int_{M_N|x_-}^{\infty} pdpd\phi \tilde{\Psi}_V^\dagger(\vec{p}_-)(1 - \vec{\alpha} \cdot \hat{q}) A^\dagger \lambda_3 A \lambda^g \Omega_g \tilde{\Psi}_V(\vec{p}_-) \\ & + \int_{M_N|x_+}^{\infty} pdpd\phi \tilde{\Psi}_V^\dagger(\vec{p}_+)(1 + \vec{\alpha} \cdot \hat{q}) \lambda^g \Omega_g A^\dagger \lambda_3 A \tilde{\Psi}_V(\vec{p}_+) | N \rangle. \end{aligned}$$

In the parton model language the assumption of a sea quark distribution which is identical for all flavors yields the historic value $S_G = 1/3$. Recent experiments by the NMC group indicate a sizable deviation $S_G = 0.235 \pm 0.026$ [42]. This has often been interpreted as an isospin violation. However, this is not the case because a non-vanishing lower component of the quark wave-function ψ_V is sufficient to provide the desired deviation from the historic value even for identical up and down quark masses [26, 28]. Since the quarks experience a mesonic background field this effect may be attributed to pion clouds [43].

4. Polarized Structure Functions

The projector suitable to extract the polarized twist-2 structure function g_1 from the hadronic tensor reads [44]

$$\Lambda_{g_1}^{\mu\nu} = \frac{2}{b} \left(2P \cdot qx S_\rho + \frac{1}{q \cdot S} \left\{ (q \cdot S)^2 - \left(\frac{P \cdot q}{M_N} \right)^2 \right\} q_\rho \right) P_\sigma \epsilon^{\mu\nu\rho\sigma} \quad (49)$$

$$\text{with } b = -4M_N \left\{ \left(\frac{P \cdot q}{M_N} \right)^2 + 2P \cdot qx - (q \cdot S)^2 \right\} \quad \text{and } \vec{s} \parallel \vec{q}. \quad (50)$$

In the Bjorken limit (33) its contraction with the hadronic tensor (27) is equivalent to the multiplication of

$$\Lambda_{g_1, \text{Bj}}^{\mu\nu} = \frac{1}{2M_N} \epsilon^{\mu\nu\lambda\tau} \frac{q_\lambda P_\tau}{q \cdot S}. \quad (51)$$

Taking into account that for g_1 the nucleon spin \vec{s} should be oriented along the photon momentum \vec{q} which is accomplished by the choice

$$\hat{q} = \hat{s} = \hat{e}_z \quad (52)$$

we obtain for this polarized structure function by repeating the computation of the previous section

$$\begin{aligned} \tilde{g}_1^{ab} &= N_C \frac{M_N}{\pi} \langle N, \hat{s} = \hat{e}_z | \int_{M_N|x_+|}^{\infty} p d p d \phi \tilde{\psi}_V^\dagger(\vec{p}_+) (1 + \alpha_3) \gamma_5 A^\dagger \mathcal{O}^{ab} A \tilde{\psi}_V(\vec{p}_+) \\ &\quad - \int_{M_N|x_-|}^{\infty} p d p d \phi \tilde{\psi}_V^\dagger(\vec{p}_-) (1 - \alpha_3) \gamma_5 A^\dagger \mathcal{O}^{ba} A \tilde{\psi}_V(\vec{p}_-) | N, \hat{s} = \hat{e}_z \rangle \\ &= \tilde{g}_{1,+}^{ab} - \tilde{g}_{1,-}^{ab} \\ \Delta g_1^{ab} &= \frac{N_C}{2\pi} \frac{d}{dx} \langle N, \hat{s} = \hat{e}_z | \int_{M_N|x_+|}^{\infty} p d p d \phi \tilde{\Psi}_V^\dagger(\vec{p}_+) (1 + \alpha_3) \gamma_5 \lambda^g \Omega_g A^\dagger \mathcal{O}^{ab} A \tilde{\Psi}_V(\vec{p}_+) \\ &\quad + \int_{M_N|x_-|}^{\infty} p d p d \phi \tilde{\Psi}_V^\dagger(\vec{p}_-) (1 - \alpha_3) \gamma_5 A^\dagger \mathcal{O}^{ba} A \Omega_g \lambda^g \tilde{\Psi}_V(\vec{p}_-) | N, \hat{s} = \hat{e}_z \rangle \\ &= \Delta g_{1,+}^{ab} + \Delta g_{1,-}^{ab}. \end{aligned} \quad (53)$$

Again we have separated the contributions arising from time dependence of the collective coordinates (29)

$$g_1^{ab} = \tilde{g}_1^{ab} + \Delta g_1^{ab}. \quad (55)$$

Of course, the flavor indices have to be chosen according to the considered process. We would like to remark that similar to the case of the unpolarized structure functions the decomposition (55) does not directly correspond to an expansion in $1/N_C$ and flavor symmetry breaking because the valence quark wave-function ψ_V contains sub-leading orders as well, *cf.* eq (28).

For the case of the electro-magnetic interaction $\mathcal{O} = \mathcal{O}^{\text{e.m.}}$, *cf.* eq (47), the sum rules discussed below are straightforwardly verified in the valence quark approximation when the previous restrictions to the inertia parameters as well as the static properties are applied. The Bjorken sum rule [45] is obtained from the difference between the first moments of the proton and neutron polarized structure functions

$$\Gamma_1^{(p)} - \Gamma_1^{(n)} = \int dx (g_1^{(p)} - g_1^{(n)}) = \frac{1}{6} g_A \quad (56)$$

with g_A being the axial (isovector) charge of the nucleon measured in neutron beta-decay. In flavor SU(3) the isosinglet charge contains octet as well as singlet pieces. The sum rule for the sum of the first moments is obtained as

$$\Gamma_1^{(p)} + \Gamma_1^{(n)} = \int dx (g_1^{(p)} + g_1^{(n)}) = \frac{5}{18} (\Delta u + \Delta d) + \frac{1}{9} \Delta s \quad (57)$$

where $\Delta q = \langle N, \hat{s} = \hat{e}_z | \bar{q} \gamma_3 \gamma_5 q | N, \hat{s} = \hat{e}_z \rangle$ refers to the nucleon matrix element of the axial current of flavor q . In this notation we have $g_A = \Delta u - \Delta d$.

The flavor singlet combination

$$\Delta u + \Delta d + \Delta s = \Sigma \quad (58)$$

corresponds to twice that part of the nucleon spin which is carried by the quarks, *i.e.* $\Sigma = 2S_q$. Its study has lead to the proton spin puzzle as the EMC [46], SMC [47] and SLAC [48, 49] measurements combined with the assumption of flavor symmetry and data from semileptonic hyperon decays indicated that Σ was unexpectedly small [11]. In addition that analysis yielded a large polarization of the strange sea in the nucleon, *i.e.* a large $\Delta s/\Delta d$. However, it was also observed that this ratio is quite sensitive to the assumption of SU(3) flavor symmetry, while the smallness of Σ remains almost unchanged once this assumption is waived [50]. Our results for Δq have already been presented in [29]. In this context it should be noted that (as long as $\delta_3 = \delta'_3$) the bilocal corrections do not alter Δq , *i.e.* $\int dx(\Delta g_{1,+}^{ab} + \Delta g_{1,-}^{ab}) = 0$.

5. Projection and DGLAP–Evolution

The structure functions of the previous sections are calculated in the nucleon (*i.e.* soliton) rest frame (RF). In the introduction we have already argued that we should transform these structure functions to the infinite momentum frame (IMF) in order to mitigate the effects originating from omitting the dynamical response⁹ of the soliton on the transferred momentum. This boost causes a Lorentz contraction [24, 25]

$$f_{\text{IMF}}(x) = \frac{\Theta(1-x)}{1-x} f_{\text{RF}}(-\ln(1-x)) \quad (59)$$

which constrains the structure functions to the interval $x \in [0, 1]$ hence providing proper support. The feature that the structure functions vanish for $x \leq 1$ is not only demanded by Lorentz covariance but also mandatory in order to include the logarithmic corrections in Q^2 employing the DGLAP evolution program [51, 52] of perturbative QCD which otherwise contained ill-defined singularities. These corrections are incorporated by integrating differential equations (*cf.* eqs (60)–(62)) for the nucleon structure functions with respect to $t = \ln(Q^2/\Lambda_{\text{QCD}}^2)$. The assumption underlying the application of the QCD evolution program to the structure functions obtained in the present model (actually any model) is that the model approximates QCD at a low scale, Q_0^2 . Hence at this scale the structure functions computed in the model and those of QCD should approximately be equal. This low scale Q_0^2 represents the initial boundary $t_0 = \ln(Q_0^2/\Lambda_{\text{QCD}}^2)$ for integrating the differential equations. It should be stressed that the lower scale Q_0^2 represents a new parameter being intrinsic to the model. We will fix Q_0^2 by demanding a best fit to the experimental data for the unpolarized structure function at the upper boundary of the t –integration. To be specific we will consider the linear combination entering the Gottfried sum rule (48). As the DGLAP procedure relies on perturbative QCD we should not take too small a value for Q_0^2 in order to stay in its range of validity. Of course, the upper boundary of the t –integration is set by the experiment to which the model results are compared.

⁹Hence the structure functions are (reference) frame-dependent quantities.

Before actually integrating the DGLAP equations the flavor singlet (s) and non-singlet (ns) pieces of the structure functions have to be disentangled as the former may also contain gluon contributions. In the notation of eq (40) the singlet component is denoted by δ_0 while both δ_3 and δ_8 are non-singlet. Formally the differential equations to be integrated read

$$\frac{df^{(\text{ns})}(x, t)}{dt} = \frac{\alpha_{\text{QCD}}(t)}{2\pi} \int_x^1 \frac{dy}{y} P_{qq} \left(\frac{x}{y} \right) f^{(\text{ns})}(y, t) , \quad (60)$$

$$\frac{df^{(0)}(x, t)}{dt} = \frac{\alpha_{\text{QCD}}(t)}{2\pi} \int_x^1 \frac{dy}{y} \left\{ P_{qq} \left(\frac{x}{y} \right) f^{(0)}(y, t) + 6P_{qg} \left(\frac{x}{y} \right) g(y, t) \right\} , \quad (61)$$

$$\frac{dg(x, t)}{dt} = \frac{\alpha_{\text{QCD}}(t)}{2\pi} \int_x^1 \frac{dy}{y} \left\{ P_{gg} \left(\frac{x}{y} \right) g(y, t) + P_{gq} \left(\frac{x}{y} \right) f^{(0)}(y, t) \right\} . \quad (62)$$

Here the quantity f symbolically represents both the unpolarized and polarized structure functions f_1 and g_1 , respectively. Note that the splitting functions P_{ij} which are listed in ref [53] differ in these two cases. At this point we have to make a further assumption as the model does not give any information about the gluon content $g(x, t_0)$ in the nucleon which arises from quarks radiating and absorbing gluons and become *visible* only as the nucleon is probed with higher photon momenta¹⁰. We hence assume that at Q_0^2 the gluon distribution function for both the unpolarized and polarized structure functions vanish. This is not unmotivated as low-scale parameterizations of the nucleon distribution functions indicate that the gluon component is indeed small [56, 57]. Hence the initial values of the integration are the model predictions of the nucleon structure functions together with $g(x, t_0) = 0$. Note that this assumption is irrelevant when determining t_0 from the unpolarized structure functions which enter the Gottfried sum rule (48) because the gluon distribution does not contribute to this isovector combination. Having carried out the DGLAP integration to the scale Q^2 , the singlet and non-singlet pieces are recombined to the physical flavor combinations. As a consequence of the evolution (62) we find non-vanishing gluon contributions to the singlet structure function at any $Q^2 > Q_0^2$.

In the numerical treatment we constrain the evolution equations to their leading order components in the QCD coupling $\alpha_{\text{QCD}}(t) = 4\pi/[(11 - 2N_f/3) \ln(Q^2/\Lambda_{\text{QCD}}^2)]$ not only for simplicity¹¹ but in particular because a next to leading order calculation requires the identification of valence and sea quark distributions at the scale Q_0^2 . This cannot be done in the present model as we merely identify the symmetries of QCD rather than the quark degrees of freedom. Note again that the valence quark level (28) is that of the NJL chiral soliton model. It is hence a constituent type quark degree of freedom and should not be confused with the valence distribution of the parton model. Actually the gap-equation (7) causes the constituent quarks to contain not only current quarks but also virtual pairs of current quarks and anti-quarks.

¹⁰However, gluonic correlations are already contained in the model which can be concluded from the non-vanishing twist-3 structure function \bar{g}_2 [26]. The QCD equations of motion can be used to show that the moments of \bar{g}_2 are matrix elements of the gluon field strength [54]. For a review on spin structure functions see ref [55].

¹¹From bag model calculations it is known that merely the variation of the model scale Q_0^2 is the major effect of taking the next to leading order correction into account [58].

Table 3: In this table we present our results for the Gottfried sum rule (48). The entries “val” and “val+vac” indicate whether only the valence quark pieces or the total values for the inertia parameters α^2, \dots, β_1 are substituted in the quantization rules (23). See also table 1.

m (MeV)	S_G		ΔS_G		$S_G + \Delta S_G$	
	val	val+vac	val	val+vac	val	val+vac
400	0.29	0.22	-0.07	-0.05	0.22	0.17
450	0.27	0.20	-0.11	-0.08	0.16	0.12

6. Discussion of Numerical Results

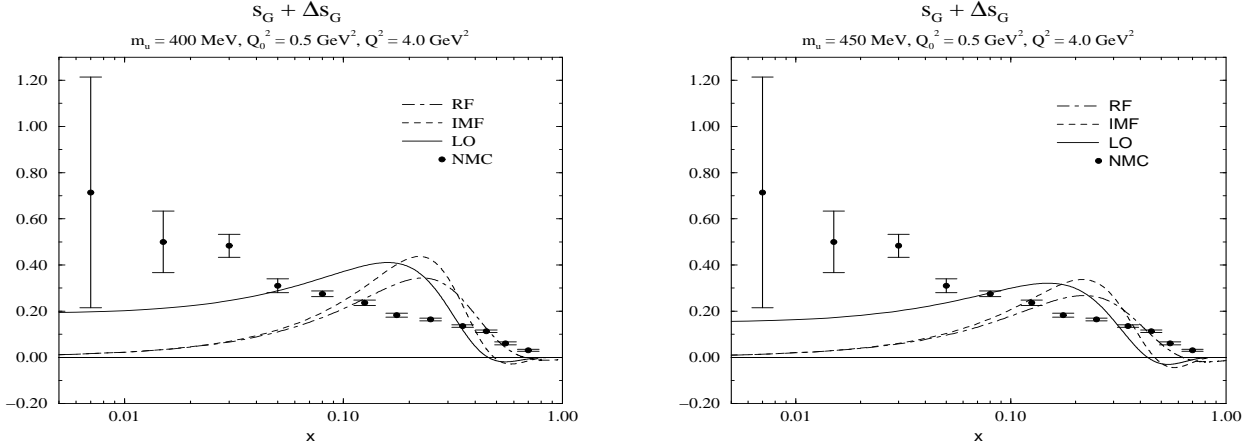
We are now prepared to compare our model predictions to the experimental data obtained for DIS at CERN and SLAC.

Within this model a reasonable description of the static properties of baryons is achieved for constituent quark masses in the range $m = 400 \dots 450 \text{ MeV}$ [3]. We will henceforth consider the two limiting values for the only free parameter in the baryon sector.

We set the stage by discussing our results for the Gottfried sum rule (46) in table 3. The value of this integral remains unchanged in the process of transforming to the IMF as well as the subsequent leading order DGLAP evolution. In presenting the results we have disentangled the two pieces associated to the integrand in eq (48). Apparently the bilocal corrections provide a sizable negative contribution; a result which was already observed in the two flavor model [39]. In table 3 the numerical results for two different calculations are shown. Those labeled by ‘val’ originate from substituting only the valence quark piece of the inertia parameters when eliminating the angular velocities in favor of SU(3) operators (23) and matrix elements (31). In this case consistency of the valence quark approximation with the Adler sum rule is maintained [26], see also section 3. The entry ‘val+vac’ refers to the inclusion of the usually significantly smaller vacuum pieces in the inertia parameters. For nucleon properties which are obtained from matrix elements of vector currents the valence quark commonly contributes to about 80% to the static properties [3] which in the case of vector charges are evidently related to the inertia parameters. For axial properties the valence level more or less saturates the static properties [3, 59]. For those reasons we consider the valence quark approximation to be most reliable when restricting to the ‘val’ prescription in the case of the unpolarized structure functions but using the total inertia parameters when later discussing the polarized structure functions. After these general remarks we return to the Gottfried sum rule and observe that for $m = 400 \text{ MeV}$ a fair agreement is obtained with the empirical value 0.235 ± 0.026 [42]. Our result for $m = 450 \text{ MeV}$ is apparently on the low side. This may be due to the valence quark approximation getting worse for larger coupling because a stronger binding of the valence quark is joined by a more pronounced polarization of the vacuum.

We proceed by comparing the integrand of the Gottfried sum rule, $s_G + \Delta s_G$ in eq (48), with the empirical data, which we assume to obey the Callan Gross relation, $f_2 = 2xf_1$. For this comparison we apply the DGLAP evolution from the model scale Q_0^2 to the scale $Q^2 = 4 \text{ GeV}^2$ at which the data are available. At Q_0^2 the integrand of the DGLAP equations is taken to be

Figure 1: Numerical results for the unpolarized structure functions entering the Gottfried sum rule for $m = 400\text{MeV}$ (left panel) and $m = 450\text{MeV}$ (right panel). Here the label RF indicates the structure functions as calculated from the expressions in the appendix, the transformation to the infinite momentum frame (59) is indicated by IMF and finally the structure functions resulting from the leading order (LO) DGLAP evolution are represented by the solid line. The empirical data are those for $(f_2^{\text{ep}} - f_2^{\text{en}})/2x$ [42]. Only the valence part of the moments of inertia enters the quantization rule.



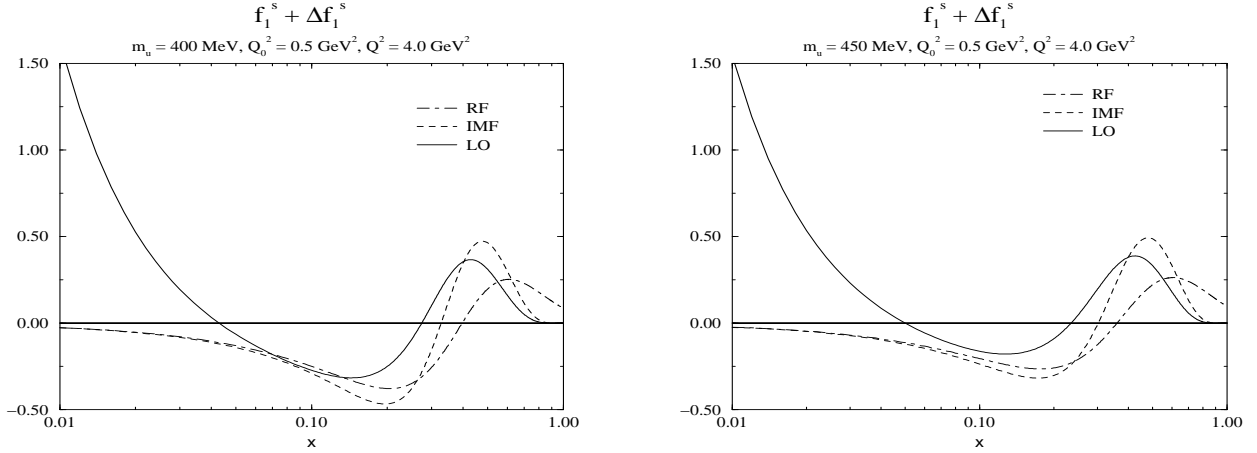
the combination $s_G + \Delta s_G$ transformed to the IMF¹². By assimilating to the overall shape of the data we determine the model scale to be $Q_0^2 \approx 0.5\text{GeV}^2$, as shown in figure 1. A smaller value for Q_0^2 might even improve on the agreement as it lowers the structure functions at large and moderate x by simultaneously increasing it at small x . However, for too small a Q_0^2 one would have to go beyond leading order in the splitting functions. As already discussed above this would require additional assumptions when identifying the model structure functions with those of QCD. From figure 1 we also note that at $x \approx 0.7$ the combination entering the Gottfried sum rule becomes slightly negative. This negative contribution is completely due to the bilocal corrections Δs_G .

Now we turn to an interesting quantity only accessible in the three flavor extension of the model: the contribution of strange degrees of freedom to the unpolarized structure function, $f_1^s(x)$. Of course, a major motivation for the present study is the investigation of quantities like $f_1^s(x)$. This structure function is obtained by setting $\mathcal{O}^{ab} = \mathcal{O}^{ba} = (1 - \sqrt{3}\lambda_8)/3$. Note that the integral over $f_1^s(x)$ is not given by the strangeness charge discussed in eq (44) as for these two quantities the pieces stemming from the backward moving quarks have opposite signs. Our results for $f_1^s(x)$ are shown in figure 2.

We observe that the structure function f_1^s exhibits a pronounced maximum at $x \approx 0.5$ after boosting the rest frame structure function to the infinite momentum frame. Naïvely one expects the momentum distribution at the low energy scale to be peaked around $x = 1/3$. However,

¹²Although the Callan Gross relation holds in our model for the structure functions at the model scale Q_0^2 it does not necessarily hold after projection and evolution. Hence we consider it appropriate to compare our results with the data obtained by applying the Callan Gross relation to the available data for f_2 .

Figure 2: Model predictions for the unpolarized structure functions of the strange projector for two different values of the constituent up quark mass. Only the valence part of the moments of inertia enters the quantization rule.

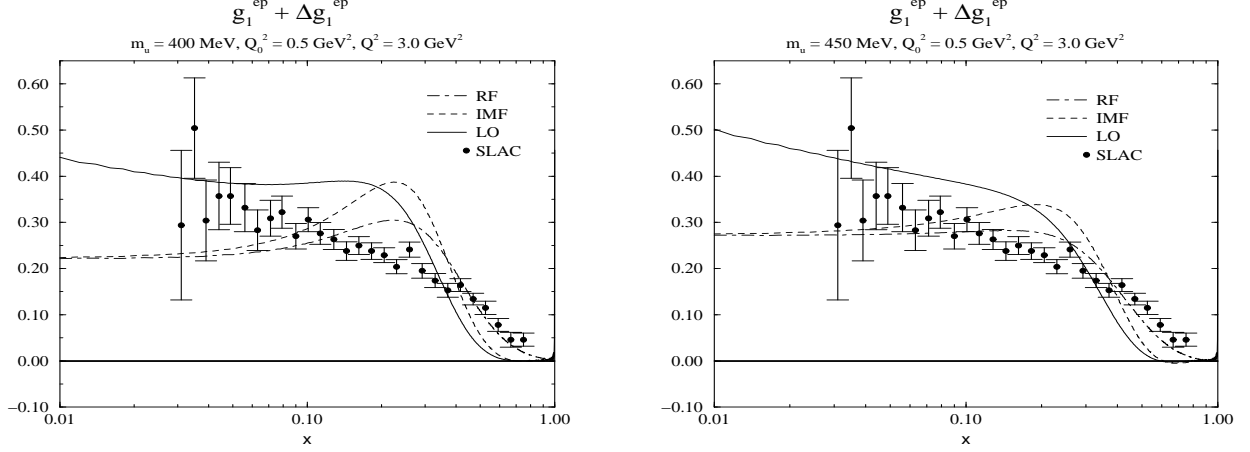


the constituent mass of strange quark is about 50% larger than that of the up or down quark, *cf.* table 1, which explains the shift of the maximum to a larger value in x . We also note that this maximum increases with the constituent mass m . This feature can be understood by recalling that this parameter actually measures the coupling of the non-strange quarks to the soliton with the soliton then exciting the strange quarks. The DGLAP evolution only leads to a moderate smearing of the maximum.

At lower x the strangeness projected unpolarized structure function becomes negative which makes a probability interpretation in the spirit of the parton model impossible. This shortcoming is most likely linked to the valence quark approximation which not only omits contributions from the polarized vacuum (which still miss the formulation of a consistent regularization) as well as certain disconnected diagrams [15] which in the background of the soliton are not necessarily disconnected. Apparently the property of a negative piece in $f_1^s(x)$ gets mitigated at higher scales as the DGLAP evolution increases this structure function at small x , it even might diverge as $x \rightarrow 0$. We would like to remark that this divergence is already present when the bilocal corrections Δf_1 are omitted [60].

As already pointed out in the introduction the polarized structure functions are of particular interest. Here we present the results for both electron-proton as well as electron-neutron scattering in figures 3 and 4, respectively. We see that after projection and DGLAP evolution the results for electron-proton scattering reproduce the gross features of the empirical data [49] for both values of the constituent quark mass $m = 400\text{MeV}$ and 450MeV . However, at moderate x the predictions slightly overestimate the data while at larger x they drop off too quickly. This might be linked to the boost into the IMF which strongly squeezes the structure functions as the comparison between the RF and IMF structure functions in figure 3 indicates. This is especially the case for smaller constituent quark masses as for those the RF structure functions are already moderately localized. Other projection procedures [61] may have a weaker

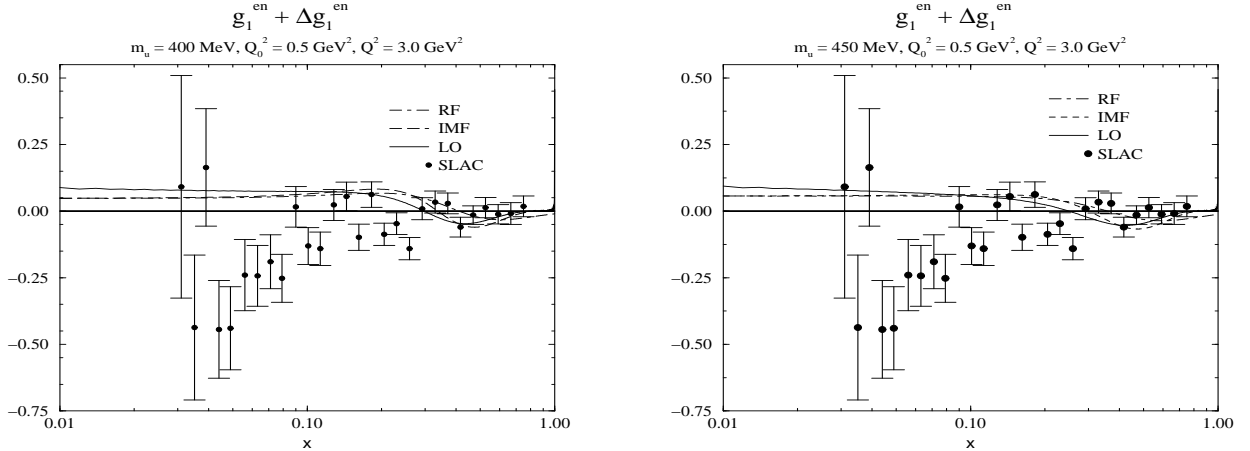
Figure 3: Numerical results for the polarized structure functions for electron–proton scattering for two different values of the constituent up–quark mass. The experimental values are taken from the SLAC E143 experiment [49]. The sum of the valence and the vacuum parts of the inertia parameters enter the quantization rule.



effect. We would also like to mention that the bilocal corrections $\Delta g_1(x)$ tend to enhance this pattern.

By taking appropriate matrix elements in eqs (53) and (54) we straightforwardly obtain the polarized structure functions for electron–neutron scattering. When comparing these results to

Figure 4: Same as figure 3 for electron–neutron scattering.

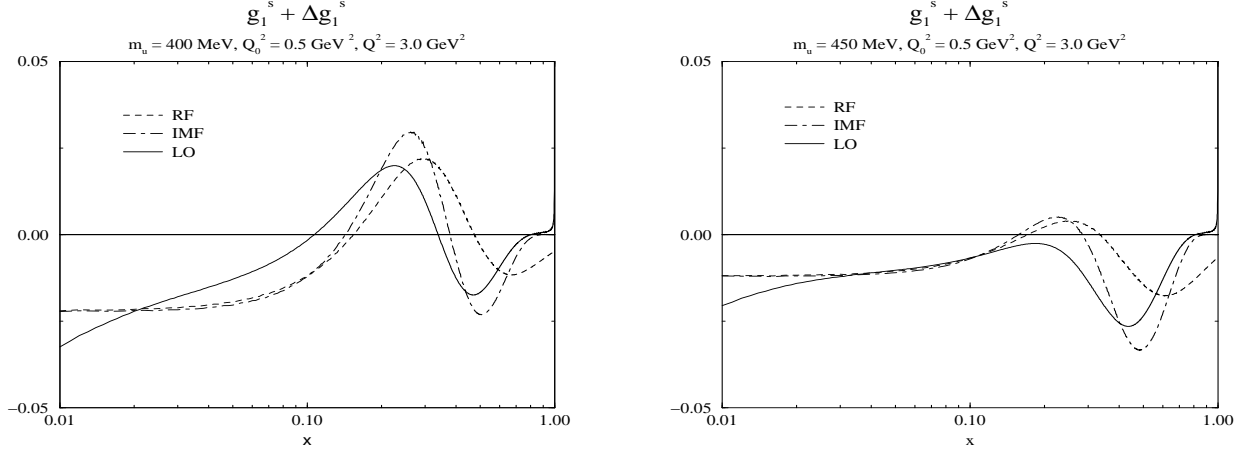


the data of the E143 experiment [49] in figure 4 we observe that the model properly reproduces the small trough in the experimental data at $x \approx 0.5$. On the other hand our model calculation does not share the tendency of most of the data to become sizable and negative at smaller x . To us it seems that the errors on the data are still too large to draw very stringent conclusions in this respect.

Finally we turn to the strange quark contribution of the polarized structure function. Again

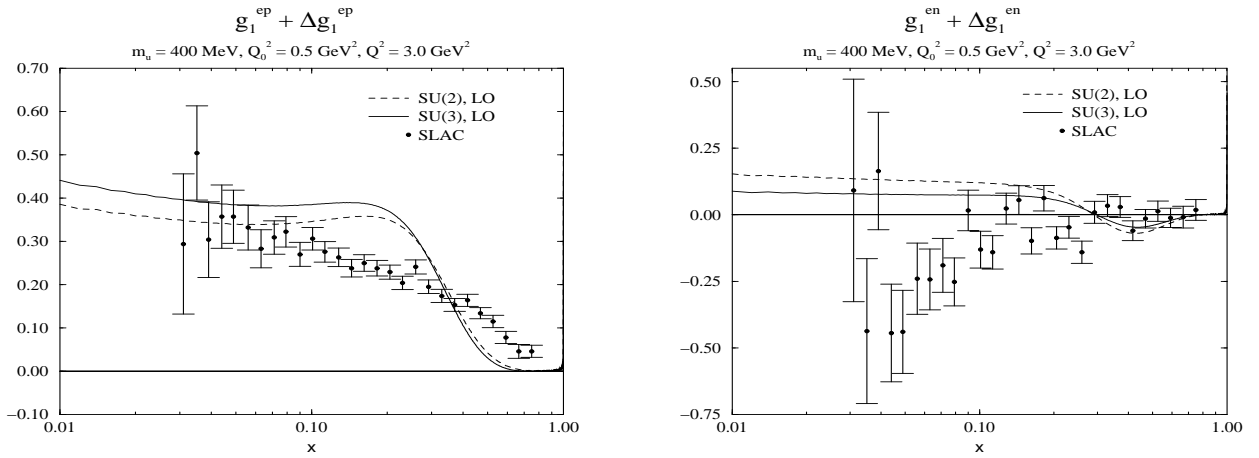
this is defined by setting $\mathcal{O}^{ab} = \mathcal{O}^{ba} = (1 - \sqrt{3}\lambda_8)/3$. Our results are shown in figure 5. These have already been presented previously [29], however, with the bilocal correction $\Delta g_1^s(x)$, which is sub-leading in $1/N_C$, omitted. The general shape of $g_1^s(x) + \Delta g_1^s(x)$ is not altered by this

Figure 5: Same as figure 2 for the polarized structure functions. Here both the valence and the vacuum part of the inertia parameters enter the expressions for the angular velocity (23,31).



additional piece. In particular the significant variation with the constituent quark mass m is maintained. We observe from figure 5 that this structure function has the strong tendency to become more negative at larger x with increasing m . In any event, we should emphasize that the magnitude of the strangeness contribution to $g_1(x)$ is quite small for all permissible parameters and the conclusion of a more or less vanishing polarization of the strange quarks in the nucleon is conceivable. The conclusion that strangeness degrees of freedom yield at most

Figure 6: Comparison with experiment [49] of the two and three flavor model predictions for the polarized structure function $g_1(x)$ of electron nucleon scattering.

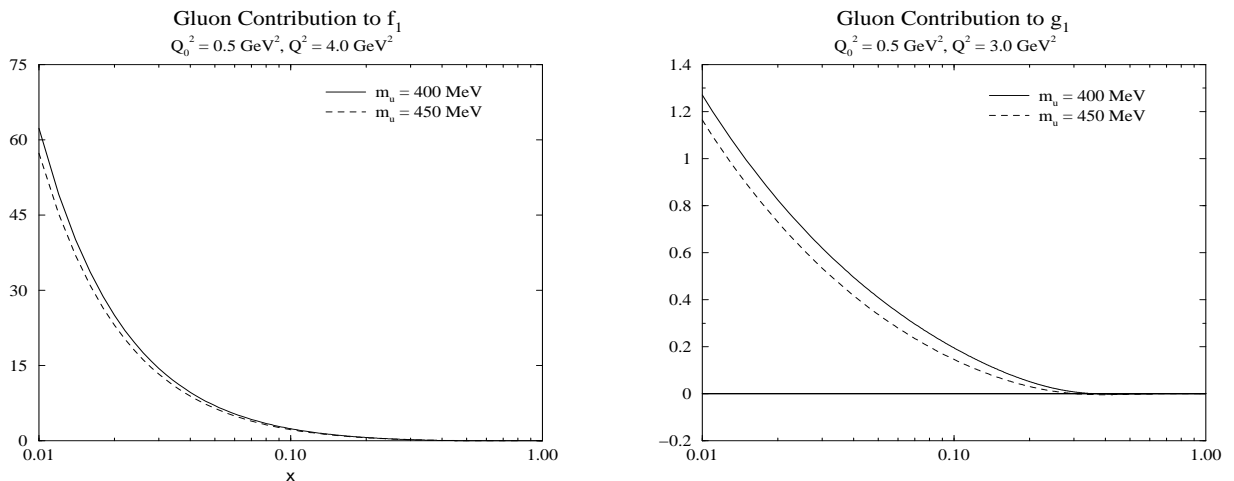


moderate effects can also be drawn from figure 6 where we compare our present results for the

polarized structure functions to those obtained in the two flavor reduction of the same model. The isoscalar combination $g_1^{\text{ep}} + g_1^{\text{en}}$ remains almost unchanged by the inclusion of strange quarks while there is a slight increase for the isovector combination $g_1^{\text{ep}} - g_1^{\text{en}}$. The fact that the latter changes at all is not only due to the additional terms (*cf.* appendix C) when extending the model to three flavors but also to the change between SU(2) and SU(3) Clebsch–Gordan coefficients arising in the calculation of nucleon matrix elements of collective operators¹³. We already communicated this result in ref [29] for the case of the polarized structure function $g_1(x)$. As can be observed from figure 1 in that reference, the use of flavor symmetric collective wave-functions enhances the difference between the extrema of $g_1(x)$ by almost a factor two.

The smallness of the strange quark contributions to the nucleon structure functions is (at least partially) due to fact that we employ a nucleon wave-function obtained by exactly diagonalizing the collective Hamiltonian. This mitigates the role of strange quarks in the nucleon [10]. We have checked that using an SU(3) symmetric wave-function yields larger strange quark pieces in the nucleon structure functions.

Figure 7: Gluon contributions to the unpolarized (left panel) and polarized (right panel) structure functions as they arise from the DGLAP evolution (62). Note the different scales for the unpolarized and polarized contributions.



For completeness we also show the gluon contributions to the structure functions at the large momentum scale Q^2 as they emerge from the DGLAP evolution (62) in figure 7. We recall that as an assumption these contributions were put to zero at the model scale Q_0^2 . Apparently the gluonic piece in the unpolarized structure function is almost two orders of magnitudes larger than in the polarized case. This huge gluonic contribution to the unpolarized structure function due to the DGLAP evolution is a well known effect. On a double logarithmic plot the unpolarized gluon distribution (times Bjorken x) grows approximately linearly as $x \rightarrow 0$ for large enough Q^2 [57]. The dependence of the gluonic pieces on the constituent quark mass apparently is negligible.

¹³When constructing the exact eigenstates of the collective Hamiltonian we employ the full inertia parameters when applying the valence quark approximation to the structure functions.

7. Conclusion

We have studied the nucleon structure functions within the three flavor Nambu–Jona–Lasinio chiral soliton model which in particular allowed us to compute the contribution of strange quarks to the structure functions.

Like in QCD, in this model the flavor symmetry is explicitly broken by different current quark masses. By the mass generation mechanism of spontaneous breaking of chiral symmetry this also induces flavor symmetry breaking for the constituent quark masses. In the baryon sector of the model the flavor symmetry breaking effects are explicitly incorporated by using an extension of the Yabu–Ando approach to quantize the chiral soliton. This yields a collective wave–function for the nucleon with good flavor and spin quantum numbers. In addition a projection onto good momentum states is performed to restore translational invariance which is broken by the soliton. Having obtained states of good momentum, the structure functions computed from a localized object are boosted to the infinite momentum frame.

Although for the construction of the chiral soliton the inclusion of the Dirac sea is mandatory, in the evaluation of the pertinent matrix elements of the hadronic tensor we use the valence quark approximation for the nucleon wave–function. This not only avoids the unsolved problem of consistently regularizing the vacuum contribution but should also be sufficient since in the chiral NJL soliton model the static properties of the nucleon are dominated or even saturated by their valence quark contribution. In this context we should emphasize, however, that in our model the valence quarks are bound constituent quarks and thus differ essentially from a valence (or sea) quark in the parton model. To minimize the ambiguities when identifying model and QCD degrees of freedom at the low energy scale where our model is supposed to approximate QCD we only use the leading order DGLAP formalism to evolve the predicted structure functions to the energy scale encountered in the corresponding experiments.

In the numeric evaluation we adjust the parameters of the model to well–known mesonic properties leaving only the constituent up quark mass as a free parameter. Note that this also determines the constituent strange quark mass. The Gottfried sum rule is fairly well reproduced for a constituent quark mass of $m = 400\text{MeV}$ but somewhat underestimated for $m = 450\text{MeV}$. This underestimation partially reflects the fact that for large constituent quark masses the contribution of the distorted vacuum becomes non–negligible (In this context one should note that the constituent quark mass represents the coupling constant between the quarks and the chiral field). The predicted unpolarized structure functions which enter the Gottfried sum rule overestimated the experimental data at large and moderate x but underestimate them at small x . A better agreement could probably be obtained by lowering the reference scale of the model in the DGLAP evolution. However, then one would have to go beyond the one leading order splitting functions.

A main focus of the present paper has been the contribution of the strange quark to the unpolarized and polarized structure functions. The strange quark part to the unpolarized structure functions $f_1^s(x)$ exhibits a pronounced peak at $x = 0.5$. The shift from the naïvely expected peak at $x = 1/3$ can be attributed to the larger mass of the strange quark. The DGLAP evolution leads only to a moderate smearing of the peak. At lower x the strangeness contribution

to the unpolarized structure functions is negative which is probably due to the valence quark approximation which ignores certain (in the vacuum) disconnected diagrams which in the presence of the chiral soliton field become connected. In general, however, the regularized vacuum contributions need not restore positivity. The DGLAP evolution substantially increases the strangeness contribution at smaller x .

After projection and DGLAP evolution the calculated polarized structure function for deep inelastic electron–proton scattering reproduces the gross features of the experimental data, although our results slightly overestimate the data at moderate x while they drop off somewhat too quickly at larger x . For electron–neutron scattering our calculated polarized structure function properly reproduces the small trough in the experimental data at $x \approx 0.5$ but fail to become sizable enough at lower x . Unfortunately the error bars on the data seem to be too large to allow for very stringent conclusions. Again, choosing a smaller reference scale of the model might improve on these deviations from the data. Our numerical results show that the strange quark contribution of the polarized structure functions is quite small and in fact conceivable with a vanishing polarization of the strange quarks in the nucleon. The comparison of the results from the two and three flavor chiral soliton model leads us to the conclusion that strange degrees of freedom yield at most moderate effects to the structure functions of the nucleon.

Acknowledgments

Helpful discussions with Leonard Gamberg are gratefully acknowledged.

A. Basis wave-functions

Although the basis states to diagonalize the quark Dirac Hamiltonian (18) in the background of the static soliton may be traced from the literature (*cf.* ref [62]) we repeat them here for completeness and use in the proceeding appendices. The eigenfunctions of this static Hamiltonian are eigenfunctions of the grand spin operator

$$\vec{G} = \vec{j} + \frac{\vec{\tau}}{2} = \vec{l} + \frac{\vec{\sigma}}{2} + \frac{\vec{\tau}}{2} \quad (63)$$

where $\vec{\tau}/2$ denotes the isospin operator in the fundamental representation. It is easily verified that \vec{G} commutes with single particle Hamiltonian (18). Additionally, the wave-functions are eigenfunctions of the parity operator. To describe the coupling of orbital angular momentum l , spin $j = l \pm 1/2$ and isospin $\tau = 1/2$ to the total grand spin G with projection quantum number M we adopt the notation

$$\mathcal{Y}_{lj}^{GM}(\hat{r}) = \langle \hat{r} | ljGM \rangle \quad \text{with} \quad |ljGM\rangle = \sum_{j_3, \tau_3} C_{jj_3 \frac{1}{2} \tau_3}^{GM} |lj j_3\rangle \Big| \frac{1}{2} \tau_3 \rangle. \quad (64)$$

The coordinate space wave-functions for the (non-strange) up and down quarks are given by

$$\Psi_{\mu}^{(G,+)}(\vec{r}) = \begin{pmatrix} ig_{\mu}^{(G,+,1)}(r) & \mathcal{Y}_{G+1/2}^{GM}(\hat{r}) \\ f_{\mu}^{(G,+,1)}(r) & \mathcal{Y}_{G+1G+1/2}^{GM}(\hat{r}) \end{pmatrix} + \begin{pmatrix} ig_{\mu}^{(G,+,2)}(r) & \mathcal{Y}_{G-1/2}^{GM}(\hat{r}) \\ -f_{\mu}^{(G,+,2)}(r) & \mathcal{Y}_{G-1G-1/2}^{GM}(\hat{r}) \end{pmatrix} \quad (65)$$

$$\Psi_{\mu}^{(G,-)}(\vec{r}) = \begin{pmatrix} ig_{\mu}^{(G,-;1)}(r) & \mathcal{Y}_{G+1G+1/2}^{GM}(\hat{r}) \\ -f_{\mu}^{(G,-;1)}(r) & \mathcal{Y}_{GG+1/2}^{GM}(\hat{r}) \end{pmatrix} + \begin{pmatrix} ig_{\mu}^{(G,-;2)}(r) & \mathcal{Y}_{G-1G-1/2}^{GM}(\hat{r}) \\ f_{\mu}^{(G,-;2)}(r) & \mathcal{Y}_{GG-1/2}^{GM}(\hat{r}) \end{pmatrix} \quad (66)$$

The superscript \pm refers to the intrinsic parity Π_{int} which is defined via total parity and the grand spin $\Pi = \Pi_{\text{int}}(-1)^G$. To discretize the quark-orbits we demand that the upper components of these spinors to vanish at the boundary of a spherical cavity with radius D ¹⁴. It should be noted that the classical part of the valence quark wave-function dwells in the $G = 0$ channel with only $j = 1/2$ being permitted:

$$\Psi_V(\vec{r}) = \begin{pmatrix} ig_V(r) & \mathcal{Y}_{0,1/2}^{00}(\hat{r}) \\ f_V(r) & \mathcal{Y}_{1,1/2}^{00}(\hat{r}) \end{pmatrix}. \quad (67)$$

As a shorthand notation to deal with the symmetry breaking corrections we introduce here the so-called *chirally rotated* radial wave-functions

$$g^{\Theta_c} = g \cos \frac{\Theta_c}{2} + f \sin \frac{\Theta_c}{2} \quad \text{and} \quad f^{\Theta_c} = f \cos \frac{\Theta_c}{2} - g \sin \frac{\Theta_c}{2} \quad (68)$$

Here Θ_c denotes the chiral angle which minimizes the classical energy (17). Since the classical soliton is embedded in the isospin subspace, the strange quarks wave-functions are those of a free Dirac field in a spherical cavity. We choose spinors with good angular momentum (*cf.* [34]):

$$\begin{aligned} s_{nl}^1(\vec{r}) &= \langle \vec{r} | 1, n, j = l + \frac{1}{2}, m \rangle = \mathcal{N}_{nl} \begin{pmatrix} i\bar{w}_{nl}^+ j_l(k_{nl}r) & \langle \vec{r} | ll + \frac{1}{2}m \rangle \\ \bar{w}_{nl}^- j_{l+1}(k_{nl}r) & \langle \vec{r} | l + 1l + \frac{1}{2}m \rangle \end{pmatrix} \\ s_{nl}^2(\vec{r}) &= \langle \vec{r} | 2, n, j = l - \frac{1}{2}, m \rangle = \mathcal{N}_{nl} \begin{pmatrix} i\bar{w}_{nl}^+ j_l(k_{nl}r) & \langle \vec{r} | ll - \frac{1}{2}m \rangle \\ -\bar{w}_{nl}^- j_{l-1}(k_{nl}r) & \langle \vec{r} | l - 1l - \frac{1}{2}m \rangle \end{pmatrix} \end{aligned}$$

with

$$\begin{aligned} E_{nl} &= \pm \sqrt{k_{nl}^2 + m_s^2} & \mathcal{N}_{nl} &= \frac{1}{D^{3/2} |j_{l+1}(k_{nl}D)|} \\ \bar{w}_{nl}^+ &= \sqrt{1 + m_s/E_{nl}}, & \bar{w}_{nl}^- &= \text{sgn}(E_{nl}) \sqrt{1 - m_s/E_{nl}}. \end{aligned}$$

Although the diagonalization of the static quark Dirac Hamiltonian operator is most conveniently performed in position space we will need the wave functions in momentum space for the computations of the structure functions. The grand spin structure will be preserved under the Fourier transformation. Generally we denote by $\tilde{R}(p)$ the Fourier transform of the radial function $R(r)$ keeping in mind that it implements a spherical Bessel function of the order of the associated orbital angular momentum, *e.g.* $\tilde{g}_{\mu}^{(G,+,1)}(p) = \int_0^D r^2 dr g_{\mu}^{(G,+,1)}(r) j_G(pr)$. For the strange quarks the situation is a bit more involved and we find it suitable to define $\tilde{s}_{nl}(k)$ as the Fourier transform involving $j_l(k_{nl}r)$ while $\tilde{t}_{nl}^1(k)$ is obtained from integrating over $j_{l+1}(k_{nl}r)$ and $\tilde{t}_{nl}^2(k)$ contains $j_{l-1}(k_{nl}r)$.

¹⁴Obviously that radius is chosen to be a multiple of the typical soliton extension.

B. Valence quark wave-function: cranking and symmetry breaking

Here we make explicit the corrections to the classical valence quark wave-function which are due to both the collective rotation h_{rot} and the flavor symmetry breaking part h_{SB} of the perturbation in eq (20) (see also eq (28)).

$$\begin{aligned} \sum_{\nu \neq V} \Psi_V \frac{\langle \nu | h_{\text{rot}} + h_{\text{SB}} | V \rangle}{\epsilon_V - \epsilon_\nu} = \\ \sum_{\mu \neq V} \Psi_\mu \left\{ \delta_{G1} \left(Q_\mu \left[\frac{\delta_{M1}}{\sqrt{2}} (\Omega_1 - i\Omega_2) - \frac{\delta_{M-1}}{\sqrt{2}} (\Omega_1 + i\Omega_2) - \delta_{M0} \Omega_3 \right] \right. \right. \\ \left. \left. + P_\mu \left[\frac{\delta_{M1}}{\sqrt{2}} (D_{81} - iD_{82}) - \frac{\delta_{M-1}}{\sqrt{2}} (D_{81} + iD_{82}) - \delta_{M0} D_{83} \right] \right) + \delta_{G0} \Gamma_\mu (D_{88} - 1) \right. \\ \left. - \frac{\mathcal{N}_{nl}/\sqrt{2}}{\epsilon_V - \epsilon_{nl}} \delta_{l0} \delta_{j\frac{1}{2}} \left(\frac{1}{2} \left[\delta_{m_j \frac{-1}{2}} (\Omega_4 + i\Omega_5) - \delta_{m_j \frac{1}{2}} (\Omega_6 + i\Omega_7) \right] \left[\bar{w}_{nl}^+ \tilde{g}_V(k_{nl}) + \bar{w}_{nl}^- \tilde{f}_V(k_{nl}) \right] \right. \right. \\ \left. \left. + \frac{m - m_s}{\sqrt{3}} \left[\delta_{m_j \frac{-1}{2}} (D_{84} + iD_{85}) - \delta_{m_j \frac{1}{2}} (D_{86} + iD_{87}) \right] \left[w_{nl}^+ \tilde{g}_V^{\Theta_c}(k_{nl}) + w_{nl}^- \tilde{f}_V^{\Theta_c}(k_{nl}) \right] \right) \right\}. \end{aligned}$$

The summation index μ runs over μ, G and $M = -G, \dots, +G$ when coupling to a non-strange spinor and over $n, j = l \pm 1/2$ and $m_j = -j, \dots, +j$ in the other case. We have used the following abbreviations for the overlap integrals:

$$\begin{aligned} Q_\mu &= \frac{1}{\epsilon_V - \epsilon_\mu} \int dr r^2 \left(g_V g_\mu^{(2,-)} + f_V f_\mu^{(2,-)} \right) \\ P_\mu &= \frac{m - m_s}{\sqrt{3}(\epsilon_V - \epsilon_\mu)} \int dr r^2 \left(g_V^{\Theta_c} g_\mu^{(2,-)\Theta_c} - f_V^{\Theta_c} f_\mu^{(2,-)\Theta_c} \right) \\ \Gamma_\mu &= \frac{m - m_s}{3(\epsilon_V - \epsilon_\mu)} \int dr r^2 \left(g_V^{\Theta_c} g_\mu^{(1,+)\Theta_c} - f_V^{\Theta_c} f_\mu^{(1,+)\Theta_c} \right) \end{aligned}$$

while the momenta k_{nl} are the roots of $j_l(k_{nl}D)$.

C. Expressions for the structure functions

In this appendix we present the expressions entering the structure function calculation using the wave-functions of the preceding appendices.

C.1 Explicit expressions for f_1

In this part we give the explicit expression for the unpolarized structure function f_1 in terms of the radial wave-functions that have been described in Appendix A. Again, g^{Θ_c} and f^{Θ_c} denote the chirally rotated wave functions.

$$\begin{aligned} f_1 &= \delta'_0 f_{1,-}^0 + \delta'_3 f_{1,-}^3 + \delta'_8 f_{1,-}^8 - \delta_0 f_{1,+}^0 - \delta_3 f_{1,+}^3 - \delta_8 f_{1,+}^8 \quad \text{with} \\ f_{1,\pm}^0 &= N_C \frac{M_N}{\pi} \langle N | \int_{M_N|x_\pm}^\infty p dp d\phi \tilde{\psi}_V^\dagger(\vec{p}_\pm) (1 \pm \alpha_3) \tilde{\psi}_V(\vec{p}_\pm) | N \rangle \\ f_{1,\pm}^l &= N_C \frac{M_N}{\pi} \langle N | \sum_{a=1}^8 D_{la} \int_{M_N|x_\pm}^\infty p dp d\phi \tilde{\psi}_V^\dagger(\vec{p}_\pm) (1 \pm \alpha_3) \lambda_a \tilde{\psi}_V(\vec{p}_\pm) | N \rangle, \quad \text{for } l = 3, 8. \end{aligned}$$

$$\begin{aligned}
f_{1,\pm}^0 &= N_C \frac{M_N}{\pi} \int_{M_N|x_{\pm}}^{\infty} pdp \left(\tilde{g}_V^2 \mp 2\tilde{f}_V \tilde{g}_V \cos \Theta^{\pm} + \tilde{f}_V^2 \right) \\
&\quad + \sum_{\mu \neq V} \Gamma_{\mu} \left[\tilde{g}_V \tilde{g}_{\mu}^{(1,+)} + \tilde{f}_V \tilde{f}_{\mu}^{(1,+)} \mp \cos \Theta^{\pm} \left(\tilde{g}_V \tilde{f}_{\mu}^{(1,+)} + \tilde{f}_V \tilde{g}_{\mu}^{(1,+)} \right) \right] \langle N|(D_{88} - 1)|N \rangle \\
f_{1,\pm}^l &= N_C \frac{M_N}{\pi} \int_{M_N|x_{\pm}}^{\infty} pdp \left\{ \left(\tilde{g}_V^2 \mp 2\tilde{f}_V \tilde{g}_V \cos \Theta^{\pm} + \tilde{f}_V^2 \right) \frac{\langle N|D_{l8}|N \rangle}{2\sqrt{3}} \right. \\
&\quad + \sum_{\mu \neq V} \left(\delta_{G0} \Gamma_{\mu} \left[\tilde{g}_V \tilde{g}_{\mu}^{(1,+)} + \tilde{f}_V \tilde{f}_{\mu}^{(1,+)} \mp \cos \Theta^{\pm} \left(\tilde{g}_V \tilde{f}_{\mu}^{(1,+)} + \tilde{f}_V \tilde{g}_{\mu}^{(1,+)} \right) \right] \langle N|D_{l8}(D_{88} - 1)|N \rangle \right. \\
&\quad + \frac{1}{2} \delta_{G1} \left[Q_{\mu} \left(B_{\mu} \mp 2N_{\mu} \cos \Theta^{\pm} \right) \langle N|D_{li}\Omega_i|N \rangle + 2P_{\mu} \left(B_{\mu} \mp 2N_{\mu} \cos \Theta^{\pm} \right) \langle N|D_{li}D_{8i}|N \rangle \right] \\
&\quad + \frac{1}{4} \delta_{l\mu 0} \frac{\mathcal{N}_{n0}^2}{\epsilon_V - \epsilon_{\mu}} \left[\left\{ \left(\bar{w}_{n0}^{+2} \tilde{g}_V(k_{n0}) \tilde{s}_{n0} + \bar{w}_{n0}^{+} \bar{w}_{n0}^{-} \tilde{f}_V(k_{n0}) \tilde{s}_{n0} \right) \left(\tilde{g}_V \pm \tilde{f}_V \cos \Theta^{\pm} \right) \right. \right. \\
&\quad \left. \left. + \left(\bar{w}_{n0}^{+} \bar{w}_{n0}^{-} \tilde{g}_V(k_{n0}) \tilde{t}_{n0}^1 + \bar{w}_{n0}^{-2} \tilde{f}_V(k_{n0}) \tilde{t}_{n0}^1 \right) \left(\tilde{f}_V \pm \tilde{g}_V \cos \Theta^{\pm} \right) \right\} \langle N|D_{l\alpha}\Omega_{\alpha}|N \rangle \right. \\
&\quad \left. + \left\{ \left(\bar{w}_{n0}^{+2} \tilde{g}_V^{\Theta^c}(k_{n0}) \tilde{s}_{n0} + \bar{w}_{n0}^{+} \bar{w}_{n0}^{-} \tilde{f}_V^{\Theta^c}(k_{n0}) \tilde{s}_{n0} \right) \left(\tilde{g}_V \pm \tilde{f}_V \cos \Theta^{\pm} \right) \right. \right. \\
&\quad \left. \left. + \left(\bar{w}_{n0}^{+} \bar{w}_{n0}^{-} \tilde{g}_V^{\Theta^c}(k_{n0}) \tilde{t}_{n0}^1 + \bar{w}_{n0}^{-2} \tilde{f}_V^{\Theta^c}(k_{n0}) \tilde{t}_{n0}^1 \right) \left(\tilde{f}_V \pm \tilde{g}_V \cos \Theta^{\pm} \right) \right\} \right. \\
&\quad \left. \left. \times \frac{2}{\sqrt{3}} (m - m_s) \langle N|D_{l\alpha}D_{8\alpha}|N \rangle \right] \right\}
\end{aligned}$$

for $l = 3, 8$ with the summation conventions $i = 1, 2, 3$ and $\alpha = 4, \dots, 7$. In case not explicitly stated, the integration variable p is the argument of \tilde{g}_V and \tilde{f}_V . We have furthermore used the following shorthand notation:

$$\begin{aligned}
B_{\mu} &= \tilde{g}_V \tilde{g}_{\mu}^{(2,-)} + \tilde{f}_V \tilde{f}_{\mu}^{(2,-)} \\
N_{\mu} &= \tilde{g}_V \tilde{f}_{\mu}^{(2,-)} + \tilde{f}_V \tilde{g}_{\mu}^{(2,-)}
\end{aligned}$$

in addition to the quantities Q_{μ} , P_{μ} and Γ_{μ} which were already introduced in appendix B.

C.2 Explicit expressions for Δf_1

As usual we split up the structure functions according to the flavor content and the two contributions from the forward and backward intermediate quark. In the case of Δf_1 this yields

$$\Delta f_1 = \delta_0 \Delta f_{1,+}^0 + \delta_3 \Delta f_{1,+}^3 + \delta_8 \Delta f_{1,+}^8 + \delta'_0 \Delta f_{1,-}^0 + \delta'_3 \Delta f_{1,-}^3 + \delta'_8 \Delta f_{1,-}^8$$

with

$$\Delta f_{1,\pm}^0 = -\frac{N_C}{2\pi} \frac{\partial}{\partial x} \int_{M_N|x_{\pm}}^{\infty} pdp \left(\tilde{f}_V(p)^2 + \tilde{g}_V(p)^2 \mp 2\tilde{f}_V(p) \tilde{g}_V(p) \cos \Theta^{\pm} \right) \left[\frac{1}{8\alpha^2} - \frac{1}{12\beta^2} \right]$$

while for $l = 3, 8$ we obtain

$$\begin{aligned}\Delta f_{1,\pm}^l &= -\frac{N_C}{2\pi} \frac{\partial}{\partial x} \int_{M_N|x_{\pm}|}^{\infty} p dp \left(\tilde{f}_V(p)^2 + \tilde{g}_V(p)^2 \mp 2\tilde{f}_V(p)\tilde{g}_V(p) \cos \Theta^{\pm} \right) \\ &\quad \left[-\frac{1}{2\alpha^2} \langle N|D_{li}(R_i + \alpha_1 D_{8i})|N \rangle - \frac{1}{4\beta^2} \langle N|D_{l\alpha}(R_{\alpha} + \beta_1 D_{8\alpha})|N \rangle \right. \\ &\quad \left. + \frac{1}{\sqrt{3}} \left(\frac{1}{8\alpha^2} - \frac{1}{12\beta^2} \right) \langle N|D_{l8}|N \rangle \right].\end{aligned}$$

C.3 Explicit expressions for g_1

In this appendix we give the explicit expression for the polarized structure function g_1 in terms of the radial wave functions that were described in Appendix A. As previously g^{Θ_c} and f^{Θ_c} denote the chirally rotated wave functions.

$$\begin{aligned}g_1 &= \delta_0 g_{1,+}^0 + \delta_3 g_{1,+}^3 + \delta_8 g_{1,+}^8 - \delta'_0 g_{1,-}^0 - \delta'_3 g_{1,-}^3 - \delta'_8 g_{1,-}^8 \quad \text{with} \\ g_{1,\pm}^0 &= N_C \frac{M_N}{\pi} \langle N| \int_{M_N|x_{\pm}|}^{\infty} p dp d\phi \tilde{\psi}_V^{\dagger}(\vec{p}_{\pm})(1 \pm \alpha_3) \gamma^5 \tilde{\psi}_V(\vec{p}_{\pm})|N \rangle \\ g_{1,\pm}^l &= N_C \frac{M_N}{\pi} \langle N| \sum_{a=1}^8 D_{la} \int_{M_N|x_{\pm}|}^{\infty} p dp d\phi \tilde{\psi}_V^{\dagger}(\vec{p}_{\pm})(1 \pm \alpha_3) \gamma^5 \lambda_a \tilde{\psi}_V(\vec{p}_{\pm})|N \rangle, \quad \text{for } l = 3, 8. \\ g_{1,\pm}^0 &= N_C \frac{M_N}{\pi} \int_{M_N|x_{\mp}|}^{\infty} p dp \sum_{\mu \neq V} \left\{ \right. \\ &\quad Q_{\mu} \left[\frac{\cos \Theta^{\pm}}{4} \left(\sqrt{2} N_{\mu}^{(1)} + N_{\mu}^{(2)} \right) \mp \frac{1}{8} \left(\sqrt{2} M_{\mu}^{(1)\pm} + M_{\mu}^{(2)\pm} \right) \right] \langle N|\Omega_3|N \rangle \\ &\quad \left. + P_{\mu} \left[\frac{\cos \Theta^{\pm}}{2} \left(\sqrt{2} N_{\mu}^{(1)} + N_{\mu}^{(2)} \right) \mp \frac{1}{4} \left(\sqrt{2} M_{\mu}^{(1)\pm} + M_{\mu}^{(2)\pm} \right) \right] \langle N|D_{83}|N \rangle \right\} \\ g_{1,\pm}^l &= N_C \frac{M_N}{\pi} \int_{M_N|x_{\pm}|}^{\infty} p dp \left\{ \left[\tilde{g}_V \tilde{f}_V \cos \Theta^{\pm} \mp \frac{1}{2} \tilde{g}_V^2 \mp \left(\cos^2 \Theta^{\pm} - \frac{1}{2} \right) \tilde{f}_V^2 \right] \langle N|D_{l3}|N \rangle \right. \\ &\quad \left. + 2 \sum_{\mu \neq V} \left(\delta_{G0} \Gamma_{\mu} \left[\frac{\cos \Theta^{\pm}}{2} \left(\tilde{g}_V \tilde{f}_{\mu}^{(1,+)} + \tilde{f}_V \tilde{g}_{\mu}^{(1,+)} \right) \mp \frac{1}{2} \tilde{g}_V \tilde{g}_{\mu}^{(1,+)} \mp \left(\cos^2 \Theta^{\pm} - \frac{1}{2} \right) \tilde{f}_V \tilde{f}_{\mu}^{(1,+)} \right] \right. \right. \\ &\quad \left. \left. \times \langle N|D_{l3}(D_{88} - 1)|N \rangle \right. \right. \\ &\quad \left. + \frac{\delta_{G1}}{\sqrt{3}} Q_{\mu} \left[\frac{\cos \Theta^{\pm}}{4} \left(\sqrt{2} N_{\mu}^{(1)} + N_{\mu}^{(2)} \right) \mp \frac{1}{8} \left(\sqrt{2} M_{\mu}^{(1)\pm} + M_{\mu}^{(2)\pm} \right) \right] \langle N|D_{l8}\Omega_3|N \rangle \right. \\ &\quad \left. + \frac{\delta_{G1}}{\sqrt{3}} P_{\mu} \left[\frac{\cos \Theta^{\pm}}{2} \left(\sqrt{2} N_{\mu}^{(1)} + N_{\mu}^{(2)} \right) \mp \frac{1}{4} \left(\sqrt{2} M_{\mu}^{(1)\pm} + M_{\mu}^{(2)\pm} \right) \right] \langle N|D_{l8}D_{83}|N \rangle \right. \\ &\quad \left. + \frac{1}{4} \frac{\mathcal{N}_{n0}^2}{\epsilon_V - \epsilon_{\mu}} \delta_{l\mu 0} \left[\left(\tilde{g}_V \cos \Theta^{\pm} \mp \frac{1}{2} \tilde{f}_V (2 \cos^2 \Theta^{\pm} - 1) \right) \right. \right. \\ &\quad \left. \left. \times \left(\bar{w}_{n0}^+ \bar{w}_{n0}^- \tilde{g}_V(k_{n0}) \tilde{t}_{n0}^1 + \bar{w}_{n0}^{-2} \tilde{f}_V(k_{n0}) \tilde{t}_{n0}^1 \right) \right. \right. \\ &\quad \left. \left. + \frac{1}{2} \left(\tilde{f}_V \cos \Theta^{\pm} \mp \tilde{g}_V \right) \left(\bar{w}_{n0}^{+2} \tilde{g}_V(k_{n0}) \tilde{s}_{n0} + \bar{w}_{n0}^+ \bar{w}_{n0}^- \tilde{f}_V(k_{n0}) \tilde{s}_{n0} \right) \right] \right. \\ &\quad \left. \times \langle N|2d_{3\alpha\beta} D_{l\alpha} \Omega_{\beta}|N \rangle \right\}\end{aligned}$$

$$\begin{aligned}
& + \frac{m - m_s}{2\sqrt{3}} \frac{\mathcal{N}_{n0}^2}{\epsilon_V - \epsilon_\mu} \left[\left(\tilde{g}_V \cos \Theta^\pm \mp \frac{1}{2} \tilde{f}_V (2 \cos^2 \Theta^\pm - 1) \right) \right. \\
& \quad \times \left(\bar{w}_{n0}^+ \bar{w}_{n0}^- \tilde{g}_V^{\Theta^c}(k_{n0}) \tilde{t}_{n0}^1 - \bar{w}_{n0}^{-2} \tilde{f}_V^{\Theta^c}(k_{n0}) \tilde{t}_{n0}^1 \right) \\
& \quad \left. + \frac{1}{2} \left(\tilde{f}_V \cos \Theta^\pm \mp \tilde{g}_V \right) \left(\bar{w}_{n0}^{+2} \tilde{g}_V^{\Theta^c}(k_{n0}) \tilde{s}_{n0} - \bar{w}_{n0}^+ \bar{w}_{n0}^- \tilde{f}_V^{\Theta^c}(k_{n0}) \tilde{s}_{n0} \right) \right] \\
& \quad \times \langle N | 2d_{3\alpha\beta} D_{l\alpha} D_{8\beta} | N \rangle \Bigg\}
\end{aligned}$$

for $l = 3, 8$. The summation involves $i = 1, 2, 3$ as well as $\alpha, \beta = 4, \dots, 7$. We have used the following shorthand notation in order to simplify the presentation

$$\begin{aligned}
N_\mu^{(j)} &= \tilde{g}_V \tilde{f}_\mu^{(j,-)} + \tilde{f}_V \tilde{g}_\mu^{(j,-)}, \quad j = 1, 2 \\
M_\mu^{(1)\pm} &= \left(\tilde{g}_V \tilde{g}_\mu^{(1,-)} (3 \cos^2 \Theta^\pm - 1) + \tilde{f}_V \tilde{f}_\mu^{(1,-)} \right) (1 + \cos^2 \Theta^\pm) \\
M_\mu^{(2)\pm} &= 2 \left(\tilde{g}_V \tilde{g}_\mu^{(2,-)} + \tilde{f}_V \tilde{f}_\mu^{(2,-)} (2 \cos^2 \Theta^\pm - 1) \right)
\end{aligned}$$

while Q_μ , P_μ and Γ_μ are again those listed already in appendix B.

C.4 Explicit expressions for Δg_1

Finally we present the formulae for the bilocal correction Δg_1 .

$$\Delta g_1 = \delta_0 \Delta g_{1,+}^0 + \delta_3 \Delta g_{1,+}^3 + \delta_8 \Delta g_{1,+}^8 + \delta'_0 \Delta g_{1,-}^3 + \delta'_3 \Delta g_{1,-}^3 + \delta'_8 \Delta g_{1,-}^8.$$

Herein the expression for the singlet is quite simple

$$\begin{aligned}
\Delta g_{1,\pm}^0 &= \frac{N_C}{2\pi} \frac{\partial}{\partial x} \int_{M_N|x_\pm}^\infty p dp \left[\cos \Theta^\pm \tilde{g}_V(p) \tilde{f}_V(p) \mp \frac{1}{2} \tilde{g}_V(p)^2 \mp (\cos^2 \Theta^\pm - \frac{1}{2}) \tilde{f}_V(p)^2 \right] \\
&\quad \times \left[\frac{1}{2\alpha^2} - \frac{\alpha_1}{\alpha^2} \langle N | D_{83} | N \rangle \right]
\end{aligned}$$

while for $l = 3, 8$ we find

$$\begin{aligned}
\Delta g_{1,\pm}^3 &= \frac{N_C}{2\pi} \frac{\partial}{\partial x} \int_{M_N|x_\pm}^\infty p dp \left[\cos \Theta^\pm \tilde{g}_V(p) \tilde{f}_V(p) \mp \frac{1}{2} \tilde{g}_V(p)^2 \mp (\cos^2 \Theta^\pm - \frac{1}{2}) \tilde{f}_V(p)^2 \right] \\
&\quad \times \left[-\frac{1}{\beta^2} \langle N | d_{3\alpha\beta} D_{3\alpha} R_\beta | N \rangle - \left(\frac{\beta_1}{\sqrt{3}\beta^2} + \frac{1}{6\beta^2} - \frac{1}{4\alpha^2} \right) \langle N | D_{33} | N \rangle \right. \\
&\quad \left. - \frac{1}{\sqrt{3}} \left(-\frac{\beta_1}{\beta^2} + \frac{\alpha_1}{\alpha^2} \right) \langle N | D_{38} D_{83} | N \rangle + \frac{\beta_1}{\sqrt{3}\beta^2} \langle N | D_{33} D_{88} | N \rangle \right. \\
&\quad \left. - \frac{1}{\sqrt{3}\alpha^2} \langle N | D_{38} R_3 | N \rangle \right],
\end{aligned}$$

$$\begin{aligned}
\Delta g_{1,\pm}^8 = & \frac{N_C}{2\pi} \frac{\partial}{\partial x} \int_{M_N|x_{\pm}|}^{\infty} p dp \left[\cos \Theta^{\pm} \tilde{g}_V(p) \tilde{f}_V(p) \mp \frac{1}{2} \tilde{g}_V(p)^2 \mp (\cos^2 \Theta^{\pm} - \frac{1}{2}) \tilde{f}_V(p)^2 \right] \\
& \times \left[-\frac{1}{\beta^2} \langle N | d_{3\alpha\beta} D_{8\alpha} R_{\beta} | N \rangle - \left(\frac{-\beta_1}{\sqrt{3}\beta^2} + \frac{1}{6\beta^2} - \frac{1}{4\alpha^2} \right) \langle N | D_{83} | N \rangle \right. \\
& \left. - \frac{1}{\sqrt{3}} \left(-2\frac{\beta_1}{\beta^2} + \frac{\alpha_1}{\alpha^2} \right) \langle N | D_{88} D_{83} | N \rangle - \frac{1}{\sqrt{3}\alpha^2} \langle N | D_{88} R_3 | N \rangle \right].
\end{aligned}$$

This completes the list of matrix elements entering our structure function calculation.

References

- [1] Y. Nambu and G. Jona-Lasinio, Phys. Rev. **122** (1961) 345; **124** (1961) 246.
- [2] H. Reinhardt and R. Wünsch, Phys. Lett. **215** (1988) 577, **B 230** (1989) 93,
T. Meißner, F. Grümmer and K. Goeke, Phys. Lett. **B 227** (1989) 296;
R. Alkofer, Phys. Lett. **B 236** (1990) 310.
- [3] For reviews see:
R. Alkofer, H. Reinhardt, and H. Weigel, Phys. Rep. **265** (1996) 139.
C. V. Christov *et al.*, Prog. Part. Nucl. Phys. **37** (1996) 91.
- [4] The three flavor extension of the NJL model is discussed in:
H. Weigel, R. Alkofer and H. Reinhardt, Nucl. Phys. **B387** (1992) 638.
- [5] D. Ebert and H. Reinhardt, Nucl. Phys. **B271** (1986) 188.
- [6] E. Witten, Nucl. Phys. **B160** (1979) 57.
- [7] T. H. R. Skyrme, Proc. R. Soc. **260** (1961) 127,
G. S. Adkins, C. R. Nappi, and E. Witten, Nucl. Phys. **B228** (1983) 552.
- [8] For reviews on the Skyrme soliton model see:
G. Holzwarth and B. Schwesinger, Rep. Prog. Phys. **49** (1986) 825.
I. Zahed and G. E. Brown, Phys. Rep. **142** (1986) 481.
- [9] The inclusion of vector mesons is reviewed in:
Ulf-G. Meißner, Phys. Rep. **161** (1988) 213.
B. Schwesinger, H. Weigel, G. Holzwarth and A. Hayashi, Phys. Rep. **173** (1989) 173.
- [10] Three flavor solitons models are discussed in:
H. Weigel, Int. J. Mod. Phys. **A11** (1996) 2419.
- [11] S. Brodsky, J. Ellis and M. Karliner, Phys. Lett. **B206** (1988) 309.
J. Schechter, A. Subbaraman and H. Weigel, Phys. Rev. **D48** (1993) 339.
- [12] G. 't Hooft, Phys. Rev. **D14** (1976) 3432.
- [13] H. Reinhardt and R. Alkofer, Phys. Lett. **B207** (1988) 482.

- [14] V. Bernard, R. L. Jaffe and Ulf-G. Meißner, Phys. Lett. **198B** (1987) 92, Nucl. Phys. **B308** (1988) 753.
- [15] R. L. Jaffe, Phys. Rev. **D11** (1975) 1953.
- [16] C. J. Benesh and G. A. Miller, Phys. Rev. **D36** (1987) 1344,
A. I. Signal and A. W. Thomas, Phys. Lett. **B211** (1988) 481,
A. W. Schreiber, A. I. Signal and A. W. Thomas, Phys. Rev. **D44** (1991) 2653,
A. W. Schreiber, P. J. Mulders, A. I. Signal and A. W. Thomas, Phys. Rev. **D45** (1992) 3069,
X. I. Song and J. S. McCarthy, Phys. Rev. **D49** (1994) 3169,
X. I. Song, Phys. Rev. **D54** (1996) 1955.
- [17] V. Sanjose and V. Vento, Phys. Lett. **B225** (1988) 15, Nucl. Phys. **A501** (1989) 481,
M. Traini, V. Vento, A. Mair and A. Zambarda, Nucl. Phys. **A614** (1997) 472.
- [18] H. Holtmann, A. Szczurek and J. Speth, Nucl. Phys. **A596** (1996) 631.
- [19] H. Meyer and P. J. Mulders, Nucl. Phys. **A528** (1991) 589,
S. A. Kulagin, W. Melnitchouck, T. Weigl and W. Weise, Nucl. Phys. **A597** (1996) 515.
- [20] H. Walliser and G. Eckart, Nucl. Phys. **A429** (1984) 514,
A. Hayashi, G. Eckart, G. Holzwarth and H. Walliser, Phys. Lett. **B147** (1984),
M. P. Mattis and M. Karliner, Phys. Rev. **D31** (1985) 2833.
- [21] C. G. Callan and I. Klebanov, Nucl. Phys. **B262** (1985) 365,
A compilation of references on heavy quark solitons may be found in:
M. Harada, F. Sannino, J. Schechter and H. Weigel, Phys. Rev. **D56** (1997) 4098.
- [22] A. D. Jackson and J. J. M. Verbaarschot, Nucl. Phys. **A484** (1988) 419,
H. Forkel *et al.*, Nucl. Phys. **A504** (1989) 818.
- [23] H. Yabu and K. Ando, Nucl. Phys. **B301** (1988) 601.
- [24] R. L. Jaffe, Phys. Lett **93B** (1980) 313, Ann. Phys. (NY) **132** (1981) 32.
- [25] L. Gamberg, H. Reinhardt and H. Weigel, Int. J. Mod. Phys. **A13** (1998) 5519.
- [26] H. Weigel, L. Gamberg and H. Reinhardt, Mod. Phys. Lett. **A11** (1996) 3021, Phys. Lett. **B399** (1997) 287, Phys. Rev. **D55** (1997) 6910.
L. Gamberg, H. Reinhardt and H. Weigel, Phys. Rev. **D58** (1998) 054014.
- [27] D. I. Diakonov *et al.*, Nucl. Phys. **B480** (1996) 341, Phys. Rev. **D56** (1997) 4069.
- [28] M. Wakamatsu and T. Kubota, Phys. Rev. **D57** (1998) 5755.
- [29] O. Schröder, H. Reinhardt and H. Weigel, Phys. Lett. **B439** (1998) 398.
- [30] S. Callan, S. Coleman, J. Wess and B. Zumino, Phys. Rev. **177** (1969) 2247.
Ö. Kaymakçalan and J. Schechter, Phys. Rev. **D31** (1985) 1109.
- [31] H. Weigel, H. Reinhardt and R. Alkofer, Phys. Lett. **B313** (1993) 377.
- [32] D. Kahana and M. Lavelle. Phys. Lett. **B298** (1993) 397.
- [33] H. Reinhardt, Nucl. Phys. **A503** (1989) 825.
- [34] R. Alkofer and H. Weigel, Comp. Phys. Comm. **82** (1994) 30.
- [35] A. Blotz *et al.*, Nucl. Phys. **A555** (1993) 765.
- [36] E. Witten, Nucl. Phys. **B223** (1983) 422, 433.
A. V. Manohar, Nucl. Phys. **B248** (1984) 19.
- [37] H. Weigel, E. Ruiz Arriola and L. Gamberg, in preparation.
- [38] R. A. Davidson and E. Ruiz Arriola, Phys. Lett. **B348** (1995) 163.
- [39] P. V. Pobylitsa *et al.*, Phys. Rev. **D59** (1999) 034024.
M. Wakamatsu and T. Kubota, hep-ph/9809443.

- [40] J. Schechter and H. Weigel, Phys. Rev. **D51** (1995) 6296.
R. Alkofer and H. Weigel, Phys. Lett. **B319** (1993) 1.
- [41] K. Gottfried, Phys. Rev. Lett. **18** (1967) 1174.
- [42] M. Arneodo *et al.* (NMC) Phys. Rev. **D50** (1994) R1.
- [43] M. Wakamatsu, Phys. Rev. **D46** (1992) 3762.
H. Walliser and G. Holzwarth, Phys. Lett. **B302** (1993) 377.
- [44] M. Anselmino *et al.*, Phys. Rep **261** (1995) 1.
- [45] J. D. Bjorken, Phys. Rev. **148** (1966) 1476.
- [46] J. Ashman *et al.*, Phys. Lett. **B206** (1988) 364, Nucl. Phys. **B328** (1989) 1.
- [47] D. Adams *et al.*, Phys. Rev. **D56** (1997) 5330.
B. Adeva *et al.*, Phys. Lett. **B412** (1997) 414.
- [48] K. Abe *et al.*, Phys. Rev. Lett. **76** (1996) 587.
- [49] K. Abe *et al.* Phys. Rev. **D58** (1998) 112003.
- [50] N. W. Park, J. Schechter and H. Weigel, Phys. Lett. **B228** (1989) 420.
R. Johnson *et al.*, Phys. Rev. **D42** (1990) 2998.
J. Lichtenstadt and H. J. Lipkin, Phys. Lett. **B353** (1995) 119.
- [51] V. N. Gribov and L. N. Lipatov, Yad. Fiz. **15** (1972) 781 [Sov. J. Nucl. Phys. **15** (1972) 438].
Y. L. Dokshitzer, Sov. Phys. JETP **46** (1977) 461.
- [52] G. Altarelli and G. Parisi, Nucl. Phys. **B126** (1977) 298.
- [53] G. Altarelli, P. Nason, and G. Ridolfi, Phys. Lett. **B320** (1994) 152, E: **B325** (1994) 538.
- [54] E. Shuryak and A. I. Vainstein, Nucl. Phys. **B201** (1982) 141.
- [55] R. L. Jaffe, “Spin, Twist and Hadron Structure...” Erice Lectures 1995, hep-ph/9602236.
- [56] M. Glück, E. Reya and A. Vogt, Z. Phys. **C67** (1995) 433.
M. Glück, E. Reya M. Stratmann and M. Vogelsang, Phys. Rev. **D53** (1996) 4775.
M. Vogelsang, Phys. Rev. **D54** (1996) 2023.
E. Ruiz Arriola, Nucl. Phys. **A641** (1998) 461.
- [57] M. Glück, E. Reya and A. Vogt, Eur. J. Phys. **C5** (1998) 461.
- [58] F. M. Steffens and A. W. Thomas, Prog. Theor. Phys. Suppl. **120** (1995) 145.
- [59] A. Blotz, M. Prasałowicz, and K. Goeke, Phys. Rev. **D53** (1996) 485.
- [60] O. Schröder, Diploma Thesis, Tübingen University 1998, unpublished.
- [61] M. Traini, A. Zambarda and V. Vento, Mod. Phys. Lett. **A10** (1995) 1235.
- [62] S. Kahana and G. Ripka, Nucl. Phys. **A429** (1984) 462.